

# Accepted Manuscript

Inflammation-Induced Expression and Secretion of MicroRNA 122 Leads to Reduced Blood Levels of Kidney-derived Erythropoietin and Anemia

Mila Rivkin, Alina Simerzin, Elina Zorde-Khvalevsky, Chofit Chai, Jonathan B. Yuval, Nofar Rosenberg, Rona Harari-Steinfeld, Ronen Schneider, Gail Amir, Reba Condiotti, Mathias Heikenwalder, Achim Weber, Christoph Schramm, Henning Wege, Johannes Kluwe, Eithan Galun, Hilla Giladi

PII: S0016-5085(16)34827-2  
DOI: [10.1053/j.gastro.2016.07.031](https://doi.org/10.1053/j.gastro.2016.07.031)  
Reference: YGAST 60604

To appear in: *Gastroenterology*  
Accepted Date: 18 July 2016

Please cite this article as: Rivkin M, Simerzin A, Zorde-Khvalevsky E, Chai C, Yuval JB, Rosenberg N, Harari-Steinfeld R, Schneider R, Amir G, Condiotti R, Heikenwalder M, Weber A, Schramm C, Wege H, Kluwe J, Galun E, Giladi H, Inflammation-Induced Expression and Secretion of MicroRNA 122 Leads to Reduced Blood Levels of Kidney-derived Erythropoietin and Anemia, *Gastroenterology* (2016), doi: 10.1053/j.gastro.2016.07.031.

This is a PDF file of an unedited manuscript that has been accepted for publication. As a service to our customers we are providing this early version of the manuscript. The manuscript will undergo copyediting, typesetting, and review of the resulting proof before it is published in its final form. Please note that during the production process errors may be discovered which could affect the content, and all legal disclaimers that apply to the journal pertain.



## **Inflammation-Induced Expression and Secretion of MicroRNA 122 Leads to Reduced Blood Levels of Kidney-derived Erythropoietin and Anemia**

Mila Rivkin<sup>1</sup>, Alina Simerzin<sup>1</sup>, Elina Zorde-Khvalevsky<sup>1</sup>, Chofit Chai<sup>1</sup>, Jonathan B. Yuval<sup>2</sup>, Nofar Rosenberg<sup>1</sup>, Rona Harari-Steinfeld<sup>1</sup>, Ronen Schneider<sup>3</sup>, Gail Amir<sup>4</sup>, Reba Condiotti<sup>5</sup>, Mathias Heikenwalder<sup>6</sup>, Achim Weber<sup>7</sup>, Christoph Schramm<sup>8</sup>, Henning Wege<sup>8</sup>, Johannes Kluwe<sup>8</sup>, Eithan Galun\*<sup>1</sup> and Hilla Giladi<sup>1</sup>

<sup>1</sup>The Goldyne Savad Institute of Gene and Cell Therapy; <sup>2</sup>Department of Surgery, <sup>3</sup>Department of Nephrology, <sup>4</sup>Department of Pathology, Hadassah Hebrew University Hospital, Ein Karem, Jerusalem, Israel; <sup>5</sup>Department of Developmental Biology and Cancer Research, Hebrew University, Hadassah Medical School; <sup>6</sup>Institute for Virology, Technische Universität München and Helmholtz Zentrum München, Munich, Germany; <sup>7</sup>Institute of Surgical Pathology, University Zurich, Zurich, Switzerland; <sup>8</sup>Department of Gastroenterology and Hepatology University Medical Center Hamburg-Eppendorf, Hamburg, Germany

\*Corresponding author:

Prof. Eithan Galun, M.D.,  
Director, Goldyne Savad Institute of Gene Therapy,  
Hadassah Hebrew University Hospital,  
Jerusalem, 91120, Israel  
Tel: 972-2-6777762;  
Fax: 972-2-6430982; email: [eithang@hadassah.org.il](mailto:eithang@hadassah.org.il)

Number of figures: 7

Conflict of interest: The authors disclose no conflicts.

### **Financial support**

Deutsche Forschungsgemeinschaft (DFG) SFB841 project C3 (E.G.), project B3 (C.S.), project B7 (J.K.); This work was supported by the I-CORE ISF center of excellence (E.G.) and the ISF grant to E.G., by the Jay Ruskin Foundation (A.S.) and by the Selma Kron Foundation to student fellowships (M.R.). Some of the human liver samples examined for this study were obtained from the “Liver.net” biobank, which was established by the Collaborative Research Centre 841 at Hamburg University Medical Center. Collection of samples and medical data was performed

after obtaining informed consent and in accordance with the regulations of the Hamburg ethics committee (PV4081).

**Author's contributions**

H.G., E.G. analyzed data, wrote Ms. M.R. performed study. E.Z., A.S., C.C., R.H., G.A., R.C., N.R. mice experiments, M.H., M.W., A.W. -NASH mice. J.Y., R.S., C.S., H.W., J.K., recruited patients.

## Abstract

**Background & Aim:** Anemia is commonly associated with acute and chronic inflammation, but the mechanisms of their interaction are not clear. We investigated whether microRNA 122 (MIR122), which is generated in the liver and is secreted into the blood, is involved in the development of anemia associated with inflammation.

**Methods:** We characterized the primary transcript of the human liver-specific *MIR122* using northern blot, quantitative real-time PCR, and 3' and 5' RACE analyses. We studied regulation of *MIR122* in human hepatocellular carcinoma (HCC) cell lines (Huh7 and HepG2) as well as in C57BL/6 and mice with disruption of the tumor necrosis factor gene (*Tnf*). Liver tissues were collected and analyzed by bioluminescence imaging or immunofluorescence. Inflammation in mice was induced by lipopolysaccharide (LPS) or by cerulein injections. Mice were given 4 successive injections of LPS, leading to inflammation-induced anemia. Steatohepatitis was induced with a choline-deficient high-fat diet. Hemolytic anemia was stimulated by phenylhydrazine injection. *MIR122* was inhibited in mice by tail-vein injection of antagomiR-122 (an oligonucleotide antagonist of *MIR122*). MicroRNA and mRNA levels were determined by quantitative real time PCR.

**Results:** The primary transcript of *MIR122* spanned 5 kb, comprising 3 exons; the third encodes *MIR122*. Within the *MIR122* promoter region we identified a nuclear factor- $\kappa$ B (NF- $\kappa$ B) binding site and demonstrated that *RELA*, as well as activators of NF- $\kappa$ B (TNF and LPS), increased promoter activity of *MIR122*. Administration of LPS to mice induced secretion of *MIR122* into blood, which required TNF. Secreted *MIR122* reached the kidney and reduced expression of erythropoietin (*Epo*), which we identified as a *MIR122* target gene. Injection of mice with antagomiR-122 increased blood levels of EPO, reticulocytes, and hemoglobin. We found an inverse relationship between blood levels of *MIR122* and EPO in mice with acute pancreatitis or steatohepatitis, and also in patients with acute inflammation.

**Conclusion:** In mice, we found that LPS-induced inflammation increases blood levels of *MIR122*, which reduces expression of *Epo* in the kidney; this is a mechanism of inflammation-induced anemia. Strategies to block *MIR122* in patients with inflammation could reduce the development or progression of anemia.

**KEY WORDS:** microbiome, NASH, mouse model, red blood cells

## Introduction

MicroRNA-122 (miR-122) is a highly abundant liver-specific microRNA whose sequence is conserved in vertebrates<sup>1</sup>. MiR-122 plays a role in cholesterol and fatty-acid metabolism<sup>2</sup>, in apoptosis<sup>3</sup>, hepatocellular carcinoma (HCC) growth<sup>4,5</sup>, and in hepatitis C virus (HCV) propagation<sup>6</sup>. MiR-122 is secreted into the blood stream and

changes in its blood level were suggested as a predictive marker for viral-, alcohol- and chemical-induced liver injury<sup>7,8</sup>.

Expression of miR-122 is regulated by a number of transcription factors including hepatocyte nuclear factors HNF1 $\alpha$ , HNF3 $\beta$ , HNF4 $\alpha$  and by C/EBP $\alpha$ <sup>9-11</sup> (CAAT/enhancer-binding protein). MiR-122 expression was also shown to be epigenetically regulated by the PPAR $\gamma$ /RXR $\alpha$  complex<sup>12</sup>. Additionally, miR-122 is regulated by Rev-ErbA alpha suggesting that miR-122 is a circadian metabolic regulator<sup>13</sup>.

Lately, NF- $\kappa$ B was found to regulate the expression of various microRNA genes<sup>14-16</sup>. NF- $\kappa$ B is a stimulatory transcription factor, controlling immunity and inflammation and important cellular processes, ranging from cell growth and differentiation to apoptosis, cancer and in particular HCC, as we have shown<sup>17</sup>. NF- $\kappa$ B consists of a family of hetero- or homo-dimers frequently including one subunit of P65 (RelA) and a second subunit such as P50, c-Rel or RelB<sup>18</sup>. Among the various stimuli responsible for NF- $\kappa$ B activation are the pro-inflammatory cytokine TNF $\alpha$  and bacterial lipopolysaccharide (LPS)<sup>19</sup>. LPS is a major membrane component of gram negative bacteria, constituting a significant fraction of the gut-microbiome bacterial population. When the lining of the intestine becomes leaky, LPS can get into the bloodstream and reach the liver through the portal system. Consequently, LPS triggers an acute-phase inflammatory response and induces anemia<sup>20</sup> by affecting the level of erythropoietin (EPO). EPO is essential for the viability and proliferation of erythrocytic progenitors and in adults, it is predominantly synthesized in the kidneys<sup>21</sup>.

We characterized the structure of the human miR-122 primary transcript and its promoter, and we demonstrate that the miR-122 promoter is enhanced by NF- $\kappa$ B ,

TNF $\alpha$  and LPS. We also show that TNF $\alpha$  and LPS enhance the secretion of miR-122 into the blood. We established that *Epo* is a target of miR-122, and upon reducing miR-122 blood levels, we could reverse anemia. Importantly, we found an inverse correlation between EPO and miR-122 levels in the blood of mice with acute and chronic inflammation and in blood of human patients with acute inflammation. This work shows that miR-122 acts like a hormone, linking the gut, liver and kidney in controlling EPO levels. Our observations are the first to show a direct link between a microRNA and inflammation-induced anemia and may constitute a basis for a novel therapeutic approach to reverse the anemic condition via reduction of miR-122 levels

## Materials and methods

### *Animal Studies*

Male and female C57BL/6 mice, 7-8 weeks old, were purchased from Harlan Laboratories (Jerusalem, Israel). *Tnf $\alpha$* -deficient mice (TNF $\alpha$  KO) in a C57BL/6 background were a gift from Dr. Moshe Sade-Feldman and Prof. Michal Baniyash (Hebrew University Jerusalem). All mice were kept in a pathogen-free facility, under a 12 h light/dark cycle. Research on mice was approved by the Hebrew University Institutional Animal Care and Ethics Committee.

### *Cell Lines and Cell Culture*

HCC-derived human cell lines: Huh7, HepG2 and Hep3B, and human non-hepatic cell lines HEK293 - embryonic kidney cells, HeLa - epithelial cells from a cervical carcinoma, P10 - Foreskin fibroblasts and U2OS - osteosarcoma cell lines, were cultured in DMEM supplemented with 10% fetal calf serum (FCS), 1% penicillin/streptomycin. Exposing a cell culture to hypoxic conditions (5% CO<sub>2</sub>, and

less than 0.1% O<sub>2</sub>) was achieved using an anaerobic jar equipped with AnaeroPack (Mitsubishi Gas Chemical, Tokyo, Japan).

### *Reagents*

LPS (E. coli 0111:B4, cat # L-2630) was purchased from Sigma-Aldrich Chemical Co., (St. Louis, MO). Recombinant human TNF $\alpha$  (210-TA) was obtained from R&D systems (Minneapolis, MN). SC-514 (50 $\mu$ M) was obtained from (Calbiochem).

Additional information is available in the Supplementary Materials and Methods section.

## **Results**

### *Characterization of the miR-122 primary transcript*

The miR-122 primary transcript, pri-miR-122, was identified in woodchuck liver tumors as a non-coding transcript named *hcr* and subsequently identified in mouse livers as a ~5 kb miR-122 precursor RNA<sup>22</sup>. We dissected pri-miR-122 from human liver RNA and found that miR-122 is generated from the third exon of pri-miR-122 which spans 5012 bases and contains 3 exons that bear typical splicing signals at the exon-intron borders (Figure 1A and Supplementary Figures 1 and 2).

### *Enhancement of miR-122 expression by NF- $\kappa$ B*

A number of transcription factors affect the expression of miR-122 (see introduction). We identified bioinformatically a putative NF- $\kappa$ B consensus sequence within the miR-122 promoter region at position -170 relative to the transcription start site (TSS). We generated a *Luciferase* reporter plasmid carrying the human miR-122

promoter from -900 to +270 bp relative to the TSS, (PmiR-122-900) (Supplementary Figure 3A) and measured its activity in various human liver-derived and non-liver cell lines. We observed high expression levels only in Huh7 cells and relatively low expression in non-hepatic cell lines (Supplementary Figure 4A). Dissecting the promoter region from the 5'-end revealed that full promoter activity was retained when the sequence extended to -250 bp upstream from the TSS (Supplementary Figure 4B). Importantly, we established that miR-122 is produced solely from the transcript generated from this promoter, using plasmids carrying the full length miR-122 genomic region, with or without this upstream promoter, and containing mutations in the pre-miR-122 region to distinguish it from endogenous miR-122 (Supplementary Figure 5).

To study the effect of NF- $\kappa$ B on miR-122 promoter activity, we co-transfected Huh7 cells with the PmiR-122-900 or -250 reporter plasmids, together with a plasmid expressing the human RelA (P65) gene. As a positive control, we used an NF- $\kappa$ B reporter plasmid. P65 enhanced significantly the miR-122 promoter of both lengths (Figure 1B).

We next tested the effect of TNF $\alpha$ , a known NF- $\kappa$ B activator, on miR-122 promoter activity. Huh7 cells were transfected with PmiR-122-900 and 24 hours later, human TNF $\alpha$  was added for 2, 6 and 24 hours, with, or without the NF- $\kappa$ B inhibitor SC-514<sup>23</sup>. Figure 1C shows that TNF $\alpha$  significantly stimulated the miR-122 promoter, and this stimulation was greatly reduced by SC-514. Similarly, TNF $\alpha$  enhancement was inhibited by another NF- $\kappa$ B inhibitor, I $\kappa$ B $\Delta$ N, a dominant-negative mutant of I $\kappa$ B<sup>24</sup> indicating that TNF $\alpha$  activation is NF- $\kappa$ B-dependent (Supplementary Figure 6A). TNF $\alpha$  did not affect the activity of the human AAT or the EF1 $\alpha$  promoters (Supplementary Figure 6B). Additionally, TNF $\alpha$  promoter

enhancement was followed by an increase in both, pri-miR-122 and mature miR-122 levels (Supplementary Figure 7).

To verify that NF- $\kappa$ B activation involves binding to the miR-122 promoter, we mutated the predicted NF- $\kappa$ B site (Figure 1D). These mutations caused significant reduction in miR-122 promoter activity and completely abolished enhancement by P65 and TNF $\alpha$  in Huh7 cells (Figure 1E and F). Furthermore, direct proof for NF- $\kappa$ B binding to the miR-122 promoter region was obtained by chromatin immunoprecipitation ChIP assay performed on Huh7 cells treated for 2 and 16 hours with TNF $\alpha$  (Supplementary Figure 14).

The NF- $\kappa$ B binding coincides with a C/EBP $\alpha$  consensus (Figure 1D), previously shown to enhance miR-122 promoter expression<sup>11</sup>. However, in our experiments, C/EBP $\alpha$  significantly repressed the activity of both, the wild type and mutated PmiR-122 promoter (Supplementary Figure 8). As a positive control for C/EBP $\alpha$  we used the IL-8 reporter plasmid which is also activated by NF- $\kappa$ B<sup>25</sup>.

We next tested the effect of LPS, a known NF- $\kappa$ B activator, on miR-122 promoter activity *in vivo*. C57Bl/6 mice were injected with plasmid PmiR-122-900 and imaged for luciferase signals one day later, and then injected i.p. with either LPS or saline, and imaged again after 3 hours, and at days 1, 2, 5, 6 and 7 post-injection. As seen in Figure 2A, LPS activated significantly the human miR-122 promoter. A second LPS injection at day 5 caused considerable re-activation. Furthermore, the plasmid carrying the mutant miR-122 promoter, when injected into mice, exhibited low activity and was only mildly induced by LPS (Figure 2B). We demonstrate that tail vein-injected reporter plasmid enters hepatocytes, using a PmiR-122 GFP reporter plasmid followed by immunostaining of liver sections for GFP (Supplementary Figure 13). MiR-122 promoter activity exhibited enhancement by LPS.

Analysis of endogenous pre-miR-122 and mature miR-122 in mice livers following LPS administration revealed enhancement of pre-miR-122 at 5 and 24 hours, whereas mature miR-122 increased significantly after 5 hours but this increase was not retained at 24 hours post LPS injection (Figure 2C and D).

### *TNF $\alpha$ and LPS enhance secretion of miR-122*

MicroRNAs, including miR-122, were found to circulate in the bloodstream<sup>26, 27</sup>. In addition, secreted microRNAs can silence their target genes in remote tissues, thereby playing a role in cell-to-cell communication<sup>28, 29</sup>.

To test whether TNF $\alpha$  also affects miR-122 secretion, we measured microRNA levels in conditioned medium of cultured Huh7 cells treated with TNF $\alpha$  for 24 hours. Figure 3A demonstrates that the growth medium of non-treated Huh7 contains a certain level of miR-122 as well as the control miR-16 and miR-18, previously shown to be secreted<sup>30, 31</sup>. Addition of TNF $\alpha$  greatly enhanced miR-122 secretion, without affecting the level of secreted miR-16 or miR-18. To eliminate the possibility that increased miR-122 secretion was due to cell death, we performed a cell proliferation assay, which demonstrated that no change in living cell numbers occurred in the TNF $\alpha$ -treated culture (Figure 3B).

To test whether LPS also induces secretion of miR-122, we injected mice i.p. with LPS and quantified miR-122 levels in plasma samples drawn before, and at 4 and 24 hours after injection. Following LPS administration, miR-122 serum levels increased already after 4 hours (4 fold) and by 24 hours, a dramatic increase was observed (Figure 3C). This increased miR-122 secretion 24 hours after LPS administration, may explain the observed decrease in mature liver miR-122 levels between 5 and 24 hours after LPS treatment (Figure 2D).

Since LPS is known to induce TNF $\alpha$  production<sup>32</sup>, we injected LPS into TNF $\alpha$  knockout (KO) mice. In these TNF $\alpha$  KO mice, LPS did not induce the secretion of miR-122 to the plasma (Figure 3D), indicating that indeed, induction of miR-122 secretion by LPS is TNF $\alpha$ -dependent. To rule out the possibility that damaged hepatocytes contributed to increased miR-122 plasma levels, we measured plasma ALT and AST enzyme levels (biomarkers of liver injury) and found no change between LPS-treated and control mice (not shown).

We next investigated whether secreted miR-122 is taken up by remote tissues 24 hours following LPS administration. The level of miR-122 was extremely low in all tissues compared to the liver, and were not significantly affected by LPS except for a significant increase observed in the kidney (Figure 3E).

### *Erythropoietin is a target of miR-122*

Our finding that LPS causes an increase in miR-122 plasma levels, prompted us to search for miR-122 target genes known to be affected by inflammation.

Bioinformatic search revealed that erythropoietin (*Epo*) is a predicted miR-122 target, carrying putative miR-122 binding sites in its 3'-UTR region; three sites in the human and two in the mouse *Epo* (Supplementary Figure 9). We cloned the 3'-UTR regions carrying two miR-122 target sites of the mouse and human *Epo* gene (sites 1+2), downstream of the luciferase gene in the pmirGLO plasmid, and used them to transfect HEK293 cells together with miR-122 or scrambled miR control. As a positive control for miR-122 activity, we used a construct carrying the 3'-UTR of AldoA, a verified miR-122 target<sup>2</sup>. A plasmid carrying the 3'-UTR of the DNMT1 gene served as a negative control. Both, the human and mouse *Epo*-3'UTR constructs demonstrated significant reduction in luciferase activity in the presence of miR-122,

similar to the AldoA reporter (Figure 4A). To further confirm that *Epo* is a true miR-122 target, we mutated the miR-122 site2 target in the human EPO 3'-UTR construct (the evolutionary conserved site) (Supplementary Figure 9D) and that diminished significantly the inhibitory effect of miR-122 on Luciferase expression (Figure 4B).

To demonstrate that miR-122 affects endogenous *Epo* mRNA levels, we transfected human HCC-derived cells, Hep3B, with miR-122 or miR-control and 24 hours later, exposed the cells to hypoxic condition, in order to increase endogenous EPO expression<sup>21</sup>. Six hours after exposure to hypoxic conditions, *Epo* mRNA levels were greatly induced and this induction was dramatically suppressed by miR-122, but was unaffected by the control microRNA, implying that *Epo* is a true miR-122 target gene (Figure 4C).

#### *The effect of miR-122 on EPO expression levels in mice*

To study the *in vivo* effect of miR-122 on EPO levels, we injected miR-122 into mice treated with phenylhydrazine (PHZ) which is known to cause lysis of RBCs, resulting in hemolytic anemia<sup>33</sup> and increased EPO levels. PHZ was injected i.p. into mice on two consecutive days and 4 days later, the mice were injected i.v. with miR-122, miR-scrambled (negative control) or siEPO (positive control). Two days after miR-122 injection, miR-122 plasma levels, as expected, were high (Supplementary Figure 10A) whereas EPO plasma levels were significantly reduced, similar to the reduction observed with siEPO, as compared to miR-control (Figure 4D).

In a reciprocal experiment, we reduced miR-122 levels by administration of antagomiR-122, (a cholesterol-modified RNA oligonucleotide<sup>2</sup>) by hydrodynamic tail vein injection, 48 hours prior to treatment with PHZ (see Supplementary Figure 10B). Inhibition of miR-122 caused a significant increase in EPO plasma levels which

was maintained for 12 days after PHZ injection (Figure 4E). An increase in reticulocyte numbers was apparent already at day 7, whereas the effect on hemoglobin levels was observed only on day 12 post- PHZ treatment. This is in line with previous observations that recovery of hemoglobin occurs more than one week following PHZ treatment<sup>34</sup>. These data substantiate the involvement of miR-122 in the regulation of EPO plasma levels following acute PHZ-induced anemia.

### *An inverse relationship between EPO and miR-122 in mice models of acute inflammation*

We wanted to assess the relationship between miR-122 and EPO levels in mice models of acute inflammation. A model of acute pancreatitis was generated by repeated i.p. injections of cerulein (a cholecystokinin analogue) into mice<sup>35</sup>. This treatment was previously shown to rapidly activate NF- $\kappa$ B<sup>36</sup>. Following cerulein injections, we observed a significant increase in mature miR-122 levels in the plasma, concomitant with reduced levels of plasma EPO levels (Figure 5A). A similar inverse miR-122/EPO relationship was also observed in the kidney (Figure 5B).

We next studied the correlation between miR-122 and EPO levels in acute inflammation induced by LPS. We injected mice with LPS and five hours later, we measured the levels of EPO, miR-122 and TNF $\alpha$  in the different tissues. As expected, mRNA levels of TNF $\alpha$  in the liver and in the kidney were greatly induced (Supplementary Figure 11A and B). LPS injection, which induces miR-122 secretion from the liver (see Figure 3C), resulted in a significant increase in the level of mature miR-122 in the kidney. In parallel, LPS induced a dramatic reduction in both, EPO mRNA levels in the kidney and EPO protein level in the blood (Figure 5C). In addition to EPO mRNA, at 5 and 24 hours after LPS injection, we observed in the

kidney, a reduction of two other miR-122 validated targets, AldoA and AGPAT1<sup>37</sup> (Figure 5D and Supplementary Figure 11C). The effect of miR-122 on its targets in the kidney was stronger at 24 hours compared to 5 hours after LPS treatment.

To further demonstrate that miR-122 is involved in the reduction of EPO levels following LPS injection, we repressed miR-122 liver levels by hydrodynamic tail vein injection of antagomiR-122, prior to LPS injection. This injection method ensures that antagomiRs reach the liver without affecting other organs<sup>38</sup>. Upon administration of antagomiR-122, plasma EPO protein level was significantly higher than that of mice injected with the control antagomiR-124. Furthermore, the kidney mRNA levels of EPO and the miR-122 targets AldoA and AGPAT1, were also significantly higher in antago-miR-122 treated mice (Figure 5E). This suggests that following LPS treatment, liver-generated circulating miR-122, reaches the kidney and regulates the expression level of its target genes, including EPO.

Further support for this hypothesis comes from our experiments in which the major source for TNF $\alpha$  production namely, macrophages and Kupffer cells, were depleted by liposome-delivered Clodronate<sup>39</sup>. As shown above (Figure 3D), LPS induction of miR-122 expression is TNF $\alpha$ -dependent. Figure 6A, depicting F4/80 immunostaining for macrophages, revealed that in mice i.p. injected with clodronate two days prior to LPS treatment, liver macrophages were abolished entirely but kidney macrophages were not affected. Accordingly, TNF $\alpha$  and IL-6 levels in the liver were greatly suppressed but not in the kidney where they were even slightly enhanced (Figure 6B). However, miR-122 levels both, in the blood and in the kidney, were significantly reduced and EPO blood levels had increased (Figure 6C,D). Concomitantly, the miR-122 target genes, AldoA and CAT-1 had increased (Figure

6E). These data suggest that the major source of miR-122 in the kidney stems from circulating blood miR-122.

### *The development of anemia following inflammation is mediated by miR-122*

In a mouse model of chronic inflammation, we analyzed the plasma of twelve months old CD-HFD mice bearing features resembling human nonalcoholic steatohepatitis (NASH), induced by long-term feeding of a Choline-Deficient-High-Fat Diet<sup>40</sup> (CD-HFD). Comparable to the acute inflammation induced by LPS and by cerulein, miR-122 levels were dramatically elevated in the plasma of these CD-HFD mice, whereas the level of EPO protein was significantly lower. Importantly, the hemoglobin level in these mice was statistically lower as compared to control mice (Figure 7A).

To demonstrate the development of anemia following LPS-induced inflammation, we treated mice with four successive injections of LPS at days 0, 2, 4 and 7 and sacrificed the mice at days 1, 6, 8 and 11. As seen in Figure 7B, hemoglobin levels were reduced significantly already at day 6 and declined further up to day 8 and gradually increased thereafter. To determine the involvement of miR-122 in the development of anemia, we inhibited miR-122 by injecting mice with antagomiR-122. As seen in Figure 7D, at five hours after LPS injection, antagomiR-122 treatment resulted in a decrease in miR-122 in the blood and in the kidney, concomitant with a significant increase in EPO plasma level. At day 7, antagomiR-122 exhibited no significant effect on EPO and miR-122 kidney levels, but still repressed miR-122 in

the blood, although to a lesser extent. Most importantly, antagomiR-122 treatment resulted in a significant increase in mice hemoglobin levels at day 7, signifying the involvement of miR-122 in the development of anemia following LPS treatment. Notably, histological analysis revealed no extramedullary hematopoiesis (not shown) and furthermore, no apparent change was observed in spleen size or weight in these treated mice (Supplementary Figure 12).

*An inverse correlation between EPO and miR-122 in human patients with acute inflammation*

To learn whether a similar inverse correlation between EPO and miR-122 is reproduced in humans with inflammation, we conducted a prospective investigation in patients with an acute bacterial infection (clinical diagnosis shown in Supplementary Table 4). Plasma samples were collected upon admission to the hospital and a few days later during hospitalization, and were analyzed for miR-122 and EPO protein levels. We observed that in 12 out of the 17 patients tested, miR-122 levels continued to rise whereas EPO levels decreased (Supplementary Table 4). These changes that occurred in the plasma levels of miR-122 and EPO during the acute infection state, exhibited a statistically significant inverse correlation, corresponding to the results observed in the inflammatory mouse models (Figure 7E).

## **Discussion**

MiR-122 exhibits pleiotropic functions in mammals. In this study we present evidence that miR-122 plays a role in inflammation-induced anemia as well. We characterized the structure of the miR-122 primary transcript and dissected the promoter region. Our analysis revealed that miR-122 is derived from the third and last

exon of a 5kb non-coding RNA, which is similar in length to the mouse pri-miR-122. It is still unknown whether the long, non-coding pri-miR-122 RNA has a function other than serving as a miR-122 precursor. We show that the pro-inflammatory mediators, LPS and TNF $\alpha$ , enhance miR-122 promoter activity through the activation of NF- $\kappa$ B and moreover, they enhance the secretion of miR-122 from the liver into the bloodstream.

We have unfolded steps linking miR-122 to inflammation-induced anemia. We demonstrate that *Epo* is a miR-122 target gene. We next show that in mice models of acute inflammation induced by LPS and cerulein, as well as in chronic inflammation in CD-HFD mice, there is induction of miR-122 secretion to the blood, concurrent with a significant decrease in EPO protein levels. Thus, an inverse correlation between EPO protein and miR-122 levels occurs in the blood upon inflammation. In addition, we observed that secreted miR-122 reached the kidney, the major site of EPO synthesis in adults, where it caused a reduction in EPO mRNA levels, as well as two other known mir-122 target genes, AldoA and AGPAT1. Furthermore, in mice injected repeatedly with LPS and in CD-HFD mice, the inverse miR-122/EPO relationship was associated with anemia.

Interestingly, our data suggest that the hepatic iron-regulatory hormone hepcidin (which is induced in response to inflammation, including LPS, and is thought to be responsible for the development of anemia of inflammation in various disease states but not in all) is not directly associated with the events leading to the inverse miR-122/EPO relationship. Importantly, miR-122 was previously shown to be a negative regulator of hepcidin<sup>46</sup>. In our CD-HFD mice, where miR-122 is induced, hepcidin liver mRNA levels were dramatically reduced. Upon Cerulein or LPS treatment, hepcidin mRNA levels increased at 6 hours but in the case of LPS, hepcidin mRNA

levels returned to the control level thereafter. As expected, inhibition of miR-122 by antagomir-122, followed by LPS injection, resulted in significant increased levels of hepcidin (Supplementary Figure 15).

Support for our proposition that the source of kidney miR-122 is from circulating blood miR-122 which originates in the liver, comes from our experiment with macrophage depletion in the liver by Clodronate. Contrary to the liver, macrophages and TNF $\alpha$  levels in the kidney were not affected and yet, miR-122 levels were significantly reduced in the kidney. In accordance, we could not detect the presence of pre-miR-122 precursor in the kidney as opposed to its high induction by LPS in the liver (Figure 2C).

Importantly, we found an inverse miR-122/EPO correlation also in blood of human patients afflicted with anemia associated with acute inflammation. In the majority of the patients tested at the acute inflammation stage and a few days later, miR-122 blood levels continued to rise whereas EPO levels were decreased.

When induction of inflammation in mice was preceded by inhibition of miR-122 by antagomiR-122 injection (known to inhibit liver miR-122), EPO plasma levels, reticulocyte number and hemoglobin levels were all restored. Based on our results, we propose a model (Figure 7F) in which inflammation that induces TNF $\alpha$ , activates NF- $\kappa$ B which in turn, induces expression and secretion of mir-122 from the liver into the blood. Circulating miR-122 then reaches the kidney where it represses EPO, eventually leading to the development of anemia.

Recombinant EPO (rhEPO) is frequently prescribed, at high amounts, to treat anemia in patients with chronic kidney disease and cancer. However, rhEPO could potentially accelerate tumor growth and jeopardize patient survival<sup>41</sup> and may also facilitate cardiovascular events. EPO and its receptor, EPOR, are expressed in many

cancers including hepatocellular carcinoma<sup>42, 43</sup>. EPO may also stimulate epithelial-mesenchymal transition (EMT) associated with cancer progression<sup>44</sup>. These risks associated with rhEPO treatment should be an incentive for developing alternative therapies.

Targeting of EPO by miR-122 is clinically significant, since it results in a concomitant reduction in red blood cell precursors and hemoglobin levels. Thus, by reducing miR-122 serum levels, endogenous EPO levels may increase. Inhibition of miR-122 can be achieved with antagomiR-122, shown in animals to have a long-term effect<sup>45</sup>. Therefore, antagomiR-122 could potentially offer a novel clinical and cost-effective therapy to reverse anemic conditions in patients and thus, substitute for the usage of rhEPO.

Our findings add additional support to the currently growing understanding that microRNAs could act as “nucleic acid hormones”. We describe the inter-organ cross-talk between the gut microbiome, the source of LPS, which induces TNF $\alpha$  in the liver to enhance miR-122, which is secreted to the blood and reaches the kidney to target EPO that consequently reduces bone marrow erythropoiesis.

In summary, our findings establish the importance of miR-122 in linking inflammatory signals to the onset of anemia thus offering a new and additional insight into the underlying mechanism of inflammation-induced anemia.

#### **ACKNOWLEDGMENTS**

We thank Dr. Moshe Sade-Feldman and Prof. Michal Baniyash for providing the TNF $\alpha$  KO mice, and Prof. Yinon Ben-Neriah for giving us the P65 and IKB $\Delta$ N expression vectors and the NF- $\kappa$ B reporter plasmid (Hebrew University, Jerusalem). Thanks to Dr. Julio Cesar Hernandez (Baylor College of Medicine, Houston) for the C/EBP $\alpha$  expression plasmid.

## References

1. Jopling C. Liver-specific microRNA-122: Biogenesis and function. *RNA Biol* 2012;9:137-42.
2. Krutzfeldt J, Rajewsky N, Braich R, Rajeev KG, Tuschl T, Manoharan M, Stoffel M. Silencing of microRNAs in vivo with 'antagomirs'. *Nature* 2005;438:685-9.
3. Lin CJ, Gong HY, Tseng HC, Wang WL, Wu JL. miR-122 targets an anti-apoptotic gene, Bcl-w, in human hepatocellular carcinoma cell lines. *Biochem Biophys Res Commun* 2008;375:315-20.
4. Coulouarn C, Factor VM, Andersen JB, Durkin ME, Thorgeirsson SS. Loss of miR-122 expression in liver cancer correlates with suppression of the hepatic phenotype and gain of metastatic properties. *Oncogene* 2009;28:3526-36.
5. **Tsai WC, Hsu PW, Lai TC**, Chau GY, Lin CW, Chen CM, Lin CD, Liao YL, Wang JL, Chau YP, Hsu MT, Hsiao M, Huang HD, Tsou AP. MicroRNA-122, a tumor suppressor microRNA that regulates intrahepatic metastasis of hepatocellular carcinoma. *Hepatology* 2009;49:1571-82.
6. **Jopling CL, Schutz S**, Sarnow P. Position-dependent function for a tandem microRNA miR-122-binding site located in the hepatitis C virus RNA genome. *Cell Host Microbe* 2008;4:77-85.
7. Wang K, Zhang S, Marzolf B, Troisch P, Brightman A, Hu Z, Hood LE, Galas DJ. Circulating microRNAs, potential biomarkers for drug-induced liver injury. *Proc Natl Acad Sci U S A* 2009;106:4402-7.
8. Bihrer V, Friedrich-Rust M, Kronenberger B, Forestier N, Hauptenthal J, Shi Y, Peveling-Oberhag J, Radeke HH, Sarrazin C, Herrmann E, Zeuzem S, Waidmann O, Piiper A. Serum miR-122 as a biomarker of necroinflammation in patients with chronic hepatitis C virus infection. *Am J Gastroenterol* 2011;106:1663-9.
9. Xu H, He JH, Xiao ZD, Zhang QQ, Chen YQ, Zhou H, Qu LH. Liver-enriched transcription factors regulate microRNA-122 that targets CUTL1 during liver development. *Hepatology* 2010;52:1431-42.
10. Li ZY, Xi Y, Zhu WN, Zeng C, Zhang ZQ, Guo ZC, Hao DL, Liu G, Feng L, Chen HZ, Chen F, Lv X, Liu DP, Liang CC. Positive regulation of hepatic miR-122 expression by HNF4alpha. *J Hepatol* 2011;55:602-11.
11. Zeng C, Wang R, Li D, Lin XJ, Wei QK, Yuan Y, Wang Q, Chen W, Zhuang SM. A novel GSK-3 beta-C/EBP alpha-miR-122-insulin-like growth factor 1 receptor regulatory circuitry in human hepatocellular carcinoma. *Hepatology* 2010;52:1702-12.
12. Song K, Han C, Zhang J, Lu D, Dash S, Feitelson M, Lim K, Wu T. Epigenetic regulation of MicroRNA-122 by peroxisome proliferator activated receptor-gamma and hepatitis b virus X protein in hepatocellular carcinoma cells. *Hepatology* 2013 58:1681-92.
13. Gatfield D, Le Martelot G, Vejnar CE, Gerlach D, Schaad O, Fleury-Olela F, Ruskeepaa AL, Oresic M, Esau CC, Zdobnov EM, Schibler U. Integration of microRNA miR-122 in hepatic circadian gene expression. *Genes Dev* 2009;23:1313-26.

14. Galardi S, Mercatelli N, Farace MG, Ciafre SA. NF- $\kappa$ B and c-Jun induce the expression of the oncogenic miR-221 and miR-222 in prostate carcinoma and glioblastoma cells. *Nucleic Acids Res* 2011;39:3892-902.
15. Boldin MP, Baltimore D. MicroRNAs, new effectors and regulators of NF- $\kappa$ B. *Immunol Rev* 2012;246:205-20.
16. Zhou R, Hu G, Gong AY, Chen XM. Binding of NF- $\kappa$ B p65 subunit to the promoter elements is involved in LPS-induced transactivation of miRNA genes in human biliary epithelial cells. *Nucleic Acids Res* 2010;38:3222-32.
17. **Pikarsky E, Porat RM, Stein I**, Abramovitch R, Amit S, Kasem S, Gutkovich-Pyest E, Urieli-Shoval S, Galun E, Ben-Neriah Y. NF- $\kappa$ B functions as a tumour promoter in inflammation-associated cancer. *Nature* 2004;431:461-6.
18. Baeuerle PA, Baltimore D. NF- $\kappa$ B: ten years after. *Cell* 1996;87:13-20.
19. Karin M, Ben-Neriah Y. Phosphorylation meets ubiquitination: the control of NF- $\kappa$ B activity. *Annu Rev Immunol* 2000;18:621-63.
20. Ballin A, Hussein A, Vaknine H, Senecky Y, Avni Y, Schreiber L, Tamary H, Boaz M. Anemia associated with acute infection in children: an animal model. *J Pediatr Hematol Oncol* 2013;35:14-7.
21. Jelkmann W. Regulation of erythropoietin production. *J Physiol* 2011;589:1251-8.
22. Chang J, Nicolas E, Marks D, Sander C, Lerro A, Buendia MA, Xu C, Mason WS, Moloshok T, Bort R, Zaret KS, Taylor JM. miR-122, a mammalian liver-specific microRNA, is processed from hcr mRNA and may downregulate the high affinity cationic amino acid transporter CAT-1. *RNA Biol* 2004;1:106-13.
23. Kishore N, Sommers C, Mathialagan S, Guzova J, Yao M, Hauser S, Huynh K, Bonar S, Mielke C, Albee L, Weier R, Graneto M, Hanau C, Perry T, Tripp CS. A selective IKK-2 inhibitor blocks NF- $\kappa$ B-dependent gene expression in interleukin-1 beta-stimulated synovial fibroblasts. *J Biol Chem* 2003;278:32861-71.
24. Lavon I, Goldberg I, Amit S, Landsman L, Jung S, Tsuberi BZ, Barshack I, Kopolovic J, Galun E, Bujard H, Ben-Neriah Y. High susceptibility to bacterial infection, but no liver dysfunction, in mice compromised for hepatocyte NF- $\kappa$ B activation. *Nat Med* 2000;6:573-7.
25. Hoffmann E, Dittrich-Breiholz O, Holtmann H, Kracht M. Multiple control of interleukin-8 gene expression. *J Leukoc Biol* 2002;72:847-55.
26. **Mitchell PS, Parkin RK, Kroh EM**, Fritz BR, Wyman SK, Pogosova-Agadjanyan EL, Peterson A, Noteboom J, O'Briant KC, Allen A, Lin DW, Urban N, Drescher CW, Knudsen BS, Stirewalt DL, Gentleman R, Vessella RL, Nelson PS, Martin DB, Tewari M. Circulating microRNAs as stable blood-based markers for cancer detection. *Proc Natl Acad Sci U S A* 2008;105:10513-8.
27. **Zhang Y, Jia Y**, Zheng R, Guo Y, Wang Y, Guo H, Fei M, Sun S. Plasma microRNA-122 as a biomarker for viral-, alcohol-, and chemical-related hepatic diseases. *Clin Chem* 2010;56:1830-8.
28. Iguchi H, Kosaka N, Ochiya T. Secretory microRNAs as a versatile communication tool. *Commun Integr Biol* 2010;3:478-81.
29. **Momen-Heravi F, Bala S**, Kodys K, Szabo G. Exosomes derived from alcohol-treated hepatocytes horizontally transfer liver specific miRNA-122 and sensitize monocytes to LPS. *Sci Rep* 2015;5:9991.

30. **Zhang Y, Liu D, Chen X**, Li J, Li L, Bian Z, Sun F, Lu J, Yin Y, Cai X, Sun Q, Wang K, Ba Y, Wang Q, Wang D, Yang J, Liu P, Xu T, Yan Q, Zhang J, Zen K, Zhang CY. Secreted monocytic miR-150 enhances targeted endothelial cell migration. *Mol Cell* 2010;39:133-44.
31. **Morimura R, Komatsu S, Ichikawa D**, Takeshita H, Tsujiura M, Nagata H, Konishi H, Shiozaki A, Ikoma H, Okamoto K, Ochiai T, Taniguchi H, Otsuji E. Novel diagnostic value of circulating miR-18a in plasma of patients with pancreatic cancer. *Br J Cancer* 2011 105:1733-40.
32. Michie HR, Manogue KR, Spriggs DR, Revhaug A, O'Dwyer S, Dinarello CA, Cerami A, Wolff SM, Wilmore DW. Detection of circulating tumor necrosis factor after endotoxin administration. *N Engl J Med* 1988;318:1481-6.
33. Criswell KA, Sulkanen AP, Hochbaum AF, Bleavins MR. Effects of phenylhydrazine or phlebotomy on peripheral blood, bone marrow and erythropoietin in Wistar rats. *J Appl Toxicol* 2000;20:25-34.
34. Cynshi O, Shimonaka Y, Higuchi M, Imai N, Suzuki H, Togashi M, Okamoto MT, Hirashima K. Effects of recombinant human erythropoietin on haemolytic anaemia in mice. *Br J Haematol* 1990;76:414-9.
35. Lampel M, Kern HF. Acute interstitial pancreatitis in the rat induced by excessive doses of a pancreatic secretagogue. *Virchows Arch A Pathol Anat Histo* 1977;373:97-117.
36. Steinle AU, Weidenbach H, Wagner M, Adler G, Schmid RM. NF-kappaB/Rel activation in cerulein pancreatitis. *Gastroenterology* 1999;116:420-30.
37. **Hsu SH, Wang B, Kota J**, Yu J, Costinean S, Kutay H, Yu L, Bai S, La Perle K, Chivukula RR, Mao H, Wei M, Clark KR, Mendell JR, Caligiuri MA, Jacob ST, Mendell JT, Ghoshal K. Essential metabolic, anti-inflammatory, and anti-tumorigenic functions of miR-122 in liver. *J Clin Invest* 2012;122:2871-83.
38. Herweijer H, Wolff JA. Gene therapy progress and prospects: hydrodynamic gene delivery. *Gene Ther* 2007;14:99-107.
39. Van Rooijen N, Sanders A. Liposome mediated depletion of macrophages: mechanism of action, preparation of liposomes and applications. *J Immunol Methods* 1994;174:83-93.
40. Wolf MJ, Adili A, Piotrowitz K, Abdullah Z, Boege Y, Stemmer K, Ringelhan M, Simonavicius N, Egger M, Wohlleber D, Lorentzen A, Einer C, Schulz S, Clavel T, Protzer U, Thiele C, Zischka H, Moch H, Tschop M, Tumanov AV, Haller D, Unger K, Karin M, Kopf M, Knolle P, Weber A, Heikenwalder M. Metabolic activation of intrahepatic CD8+ T cells and NKT cells causes nonalcoholic steatohepatitis and liver cancer via cross-talk with hepatocytes. *Cancer Cell* 2014;26:549-64.
41. Cao Y. Erythropoietin in cancer: a dilemma in risk therapy. *Trends Endocrinol Metab* 2013;24:190-9.
42. Morais C, Johnson DW, Vesey DA, Gobe GC. Functional significance of erythropoietin in renal cell carcinoma. *BMC Cancer* 2013;13:14.
43. Ribatti D, Marzullo A, Gentile A, Longo V, Nico B, Vacca A, Dammacco F. Erythropoietin/erythropoietin-receptor system is involved in angiogenesis in human hepatocellular carcinoma. *Histopathology* 2007;50:591-6.
44. Hadland BK, Longmore GD. Erythroid-stimulating agents in cancer therapy: potential dangers and biologic mechanisms. *J Clin Oncol* 2009;27:4217-26.

45. Stenvang J, Petri A, Lindow M, Obad S, Kauppinen S. Inhibition of microRNA function by antimiR oligonucleotides. *Silence* 2012;3:1.
46. Castoldi M, Vujic Spasic M, Altamura S, Elmen J, Lindow M, Kiss J, Stolte J, Sparla R, D'Alessandro LA, Klingmuller U, Fleming RE, Longerich T, Grone HJ, Benes V, Kauppinen S, Hentze MW, Muckenthaler MU. The liver-specific microRNA miR-122 controls systemic iron homeostasis in mice. *J Clin Invest* 2011;121:1386-96.

**Author names in bold designate shared co-first authors.**

## Figure Legends

**Figure 1.** Enhancement of miR-122 by NF- $\kappa$ B and TNF $\alpha$ . **(A)** A schematic presentation of pri-miR-122 with the sizes of the 3 exons and the introns and its coordinates in the USCS 2013/hg38 assembly. **(B)** The effect of RelA on miR-122 promoter activity. Huh7 cells were co-transfected with miR-122 promoter reporter plasmids PmiR-122-900 or PmiR-122-250, or an NF- $\kappa$ B reporter plasmid (NF- $\kappa$ B), together with a plasmid expressing the P65 gene (RelA). Luciferase (Luc) activity was measured 48hrs after transfection. **(C)** Enhancement of miR-122 promoter by TNF $\alpha$  is NF- $\kappa$ B dependent. Huh7 cells transfected with PmiR-122-250 were treated 24hrs later with TNF $\alpha$  (5ng/ml). The SC-514 NF- $\kappa$ B inhibitor (50  $\mu$ M) was added 45 minutes before the addition of TNF $\alpha$ . Luciferase activity was measured at the indicated times after TNF $\alpha$  addition. **(D)** The sequence of the putative NF- $\kappa$ B-C/EBP $\alpha$  site in the miR-122 promoter and the 3 mutations that were introduced therein. **(E and F)** Relative Luciferase activity in Huh7 cells transfected with the wild type (wt) or mutated (mut) PmiR-122 plasmids, and either co-transfected with the P65-expressing plasmid **(E)**, or treated one day after transfection with TNF $\alpha$  for 24hrs **(F)**. Luciferase activity was measured 48hrs after transfection and normalized to Renilla Luciferase activity expressed from a co-transfected pRL plasmid. Error bars = SD. \*P< 0.05; \*\*P< 0.01.

**Figure 2.** LPS enhances miR-122 expression. **(A)** Induction of the miR-122 promoter by LPS. Mice were i.v. hydrodynamically injected with PmiR-122-900 and one day later (day 0) imaged for luciferase activity. LPS (1mg/kg) was then injected i.p. and the mice were imaged 3hrs later and at the following 1, 2, 5, 6 and 7 days. A second LPS injection was administered at day 5. Control mice were injected with saline. Shown are images of luciferase activity in representative mice and the quantification of liver luciferase activity from the imaging data, expressed as the ratio between LPS-injected and control, saline-injected, mice (n=7). **(B)** LPS activates the miR-122 promoter in an NF- $\kappa$ B-dependent manner. Quantification of imaging data of mice hydrodynamically injected with reporter plasmids carrying the wt or mutant PmiR-122-900 promoter, and 1 day later, injected i.p. with LPS and imaged 24hrs thereafter (n=3). **(C,D)** LPS induces Pre-miR-122 **(C)** and mature miR-122 **(D)** levels determined by qRT-PCR on liver RNA extracted from mice 5 and 24hrs after injection of LPS or saline (Control) (n=5). Mature miR-122 was normalized to RNU-6, pri-miR-122 and pre-miR-122 levels were normalized to HPRT. Error bars = SD. \*P< 0.05; \*\*P< 0.01.

**Figure 3.** TNF $\alpha$  and LPS induce secretion of miR-122. **(A)** qRT-PCR analysis of miR-122 performed on RNA extracted from the culture medium of Huh7 cells treated with TNF $\alpha$  for 24hrs. **(B)** Cell proliferation assay performed on the culture medium of TNF $\alpha$ -treated Huh7 cells using the CellTiter96 kit. Doxorubicin (2  $\mu$ g/ml) (DOX) was used as a positive control for cell death. **(C-E)** qRT-PCR analysis of miR-122 performed on RNA extracted from: **(C)** plasma taken from mice treated with LPS for 4 and 24hrs; **(D)** plasma of wild type C57BL/6 (WT) or

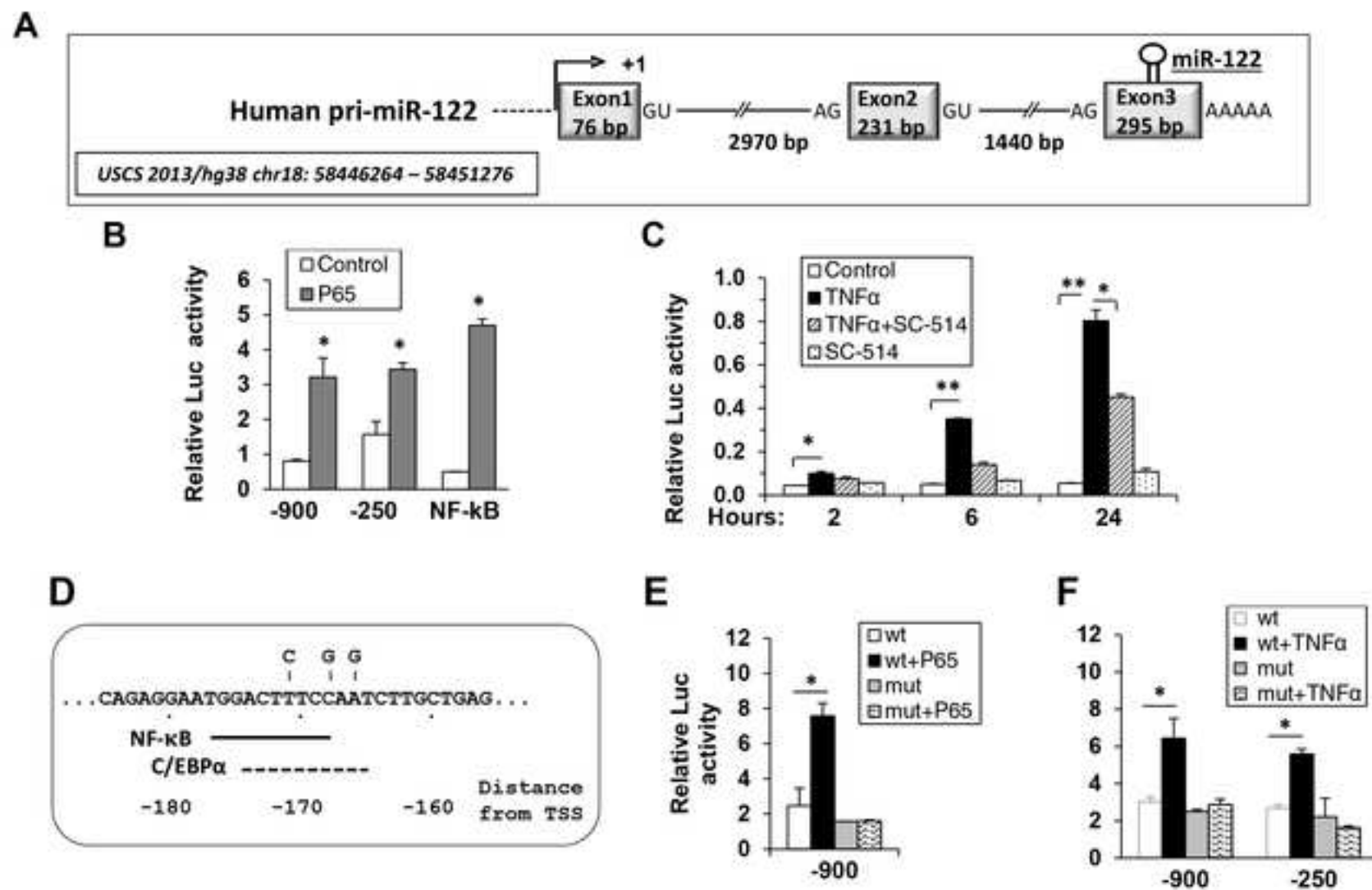
TNF $\alpha$  KO mice analyzed 24hrs after LPS or saline (Control) injection; **(E)** RNA from various tissues extracted 24hrs after LPS injection (n=4). Tissue miR-122 level was normalized to RNU-6; plasma and medium miR-122 was normalized to spiked-in cel-miR-39. Error bars = SD. \*P<0.05; \*\*P<0.01.

**Figure 4.** Erythropoietin (EPO) is a miR-122 target gene. **(A)** HEK293 cells were co-transfected with the mouse EPO 3'-UTR (mEPO) or human (hEPO) reporter plasmids, together with 50nM miR-122 (miR-122) or scrambled miR (miR-con). Reporter plasmids carrying the AldoA or the DNMT1 3'-UTR served as positive and negative controls, respectively. **(B)** HEK293 cells were transfected with reporter plasmids carrying the WT or mutated (Mut) human EPO 3'-UTR together with miR-122 or miR-con. Luciferase assays were performed 48 hours after transfection (normalized to Renilla Luciferase activity). **(C)** Hep3B cells were transfected with miR-122 or with scrambled miR and 24hrs after transfection, transferred to hypoxic conditions for 6hrs and RNA was then extracted and analyzed for EPO mRNA levels by qRT-PCR. **(D-E)** The effect of miR-122 on hemoglobin, reticulocytes, and EPO blood levels in mice treated with Phenylhydrazine (PHZ). **(D)** EPO plasma levels in PHZ-treated mice. Mice injected i.p. on two successive days with PHZ (30 mg/kg) or with saline (NT). After 4 days, mice were injected i.v. with 0.1mg/mouse of miR-scrambled (miR-con), miR-122 or siEPO. Two days after miR injection, plasma EPO levels were measured using the Quantikine ELISA kit. **(E)** Mice were hydrodynamically injected with antagomiR-122 or control antagomiR-124 two days before treatment with PHZ. At the indicated days after PHZ treatment, blood was taken for measurements of EPO protein levels, % reticulocytes and hemoglobin (HB) levels (n=5). Error bars = SD. \*P<0.05; \*\*P<0.01.

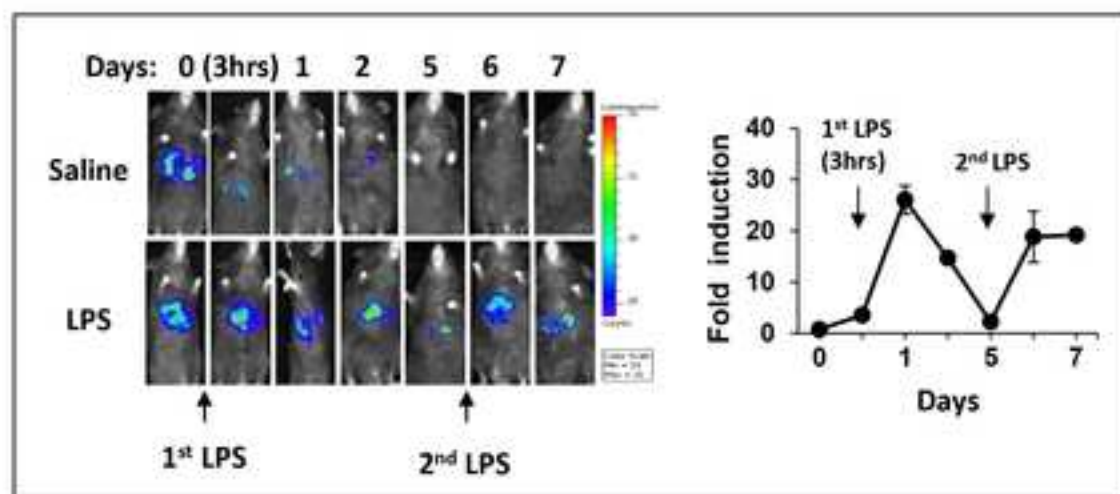
**Fig. 5.** Inverse correlation between miR-122 and EPO levels in mice models of acute inflammation. **(A,B)** Cerulein model. Mice were induced for acute pancreatitis by cerulein treatment (Cerulein) involving 6 successive i.p. hourly injections (50  $\mu$ g/kg) and were sacrificed 1 hour after the last injection for measurement of plasma miR-122 and EPO protein levels **(A)** and for kidney miR-122 and EPO mRNA levels **(B)** (n=6). Control mice (Con) were injected with saline. **(C)** LPS model. Wild type C57BL/6 mice were injected i.p. with LPS (1 mg/kg) or saline (Control) and 5 hours later, RNA was extracted from the kidneys for qRT-PCR analysis of mature miR-122 and EPO mRNA levels and blood was taken for measurement of EPO protein level (n=4). **(D)** qRT-PCR analysis of kidney mRNA levels of EPO and the miR-122 validated targets AldoA and AGPAT1 measured 24hrs after LPS injection. RPL4 served as a negative control gene. **(E)** The effect of miR-122 inhibition by antagomiR-122. C57BL/6 mice were tail-vein injected with antagomiR-122 (Ant-122) or control antagomiR-124 (Ant-124) (5 $\mu$ g/mouse) and 24hrs later, injected i.p. with LPS. 24hrs after LPS injection blood was taken for EPO protein measurement and RNA extracted from the kidneys for qRT-PCR analysis of the mRNA levels of EPO, AldoA and AGPAT1. Error bars = SD. \*P<0.05; \*\*P<0.01; \*\*\*P<0.001.

**Fig. 6.** The effect of liver macrophage depletion on miR-122 plasma and kidney levels. Analysis of liver and kidney tissues taken 5hrs after LPS treatment from mice injected, 2 days prior to LPS-treatment, with Clodronate (LPS Clodronate) or PBS (LPS Control) (n=4). **(A)** F4/80 immunostaining of liver and kidney macrophages. **(B)** qRT-PCR analysis of TNF $\alpha$  and IL-6 mRNAs in the liver and kidney. **(C)** qRT-PCR analysis of plasma and kidney miR levels. miR-16 and miR-18 served as negative controls. **(D)** EPO protein levels in the plasma. **(E)** qRT-PCR of the miR-122 targets AldoA and CAT-1 in kidney. Error bars = SD. \*P< 0.05; \*\*P<0.01; \*\*\*P<0.001.

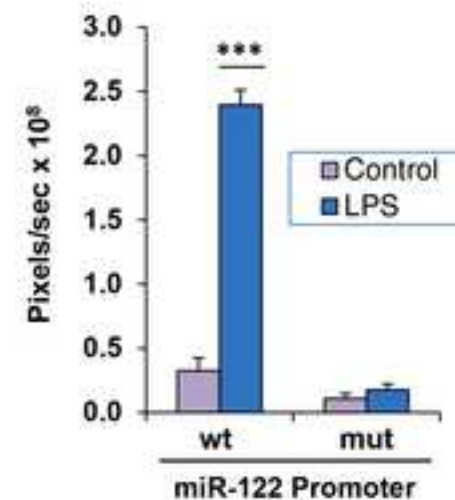
**Fig. 7.** Inflammation-induced anemia is mediated by miR-122. **(A)** Chronic inflammation model. Blood samples taken from 12 months old CD-HFD C57BL/6 mice (HFD) or from mice fed a normal diet (Con), for measurements of plasma EPO protein and miR-122 levels, as well as blood hemoglobin level (n=5). **(B)** LPS model of inflammation-induced anemia. Mice were i.p. injected with LPS (0.5mg/kg) for four successive injections at days 0, 2, 4 and 7. Blood hemoglobin levels were determined at day 1, 6, 8 and 11 after the first LPS injection (n=6). **(C,D)** The effect of miR-122 inhibition by antagomiR on LPS-induced anemia. **(C)** Experimental design: mice were i.v. hydrodynamically injected with antagomiR-122 or antagomiR-Scr control (5 $\mu$ g/mouse) 3 days before and one day after the first LPS injection. Two additional LPS injections were administered at days 2 and 4. **(D)** Mice were sacrificed at 5hrs after the first LPS and at day 7 and analyzed for miR-122 and EPO plasma levels and for miR-122 kidney levels. Hemoglobin was measured at day 7. **(E)** Correlation analysis between changes in plasma EPO protein ( $\Delta$  EPO) and miR-122 ( $\Delta$  miR-122) levels measured during patient hospitalization for acute inflammation (Pearson correlation analysis  $r = -0.6415$ ;  $P=0.0074$ ) (see supplementary Table 4). Error bars = SD. \*P< 0.05; \*\*P<0.01; \*\*\*P<0.001. **(F)** schematic presentation of our model of the involvement of miR-122 in inflammation-induced anemia.



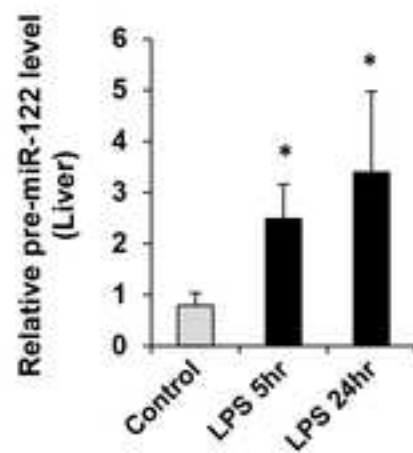
A



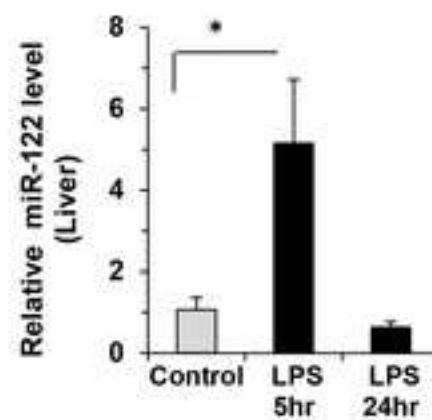
B

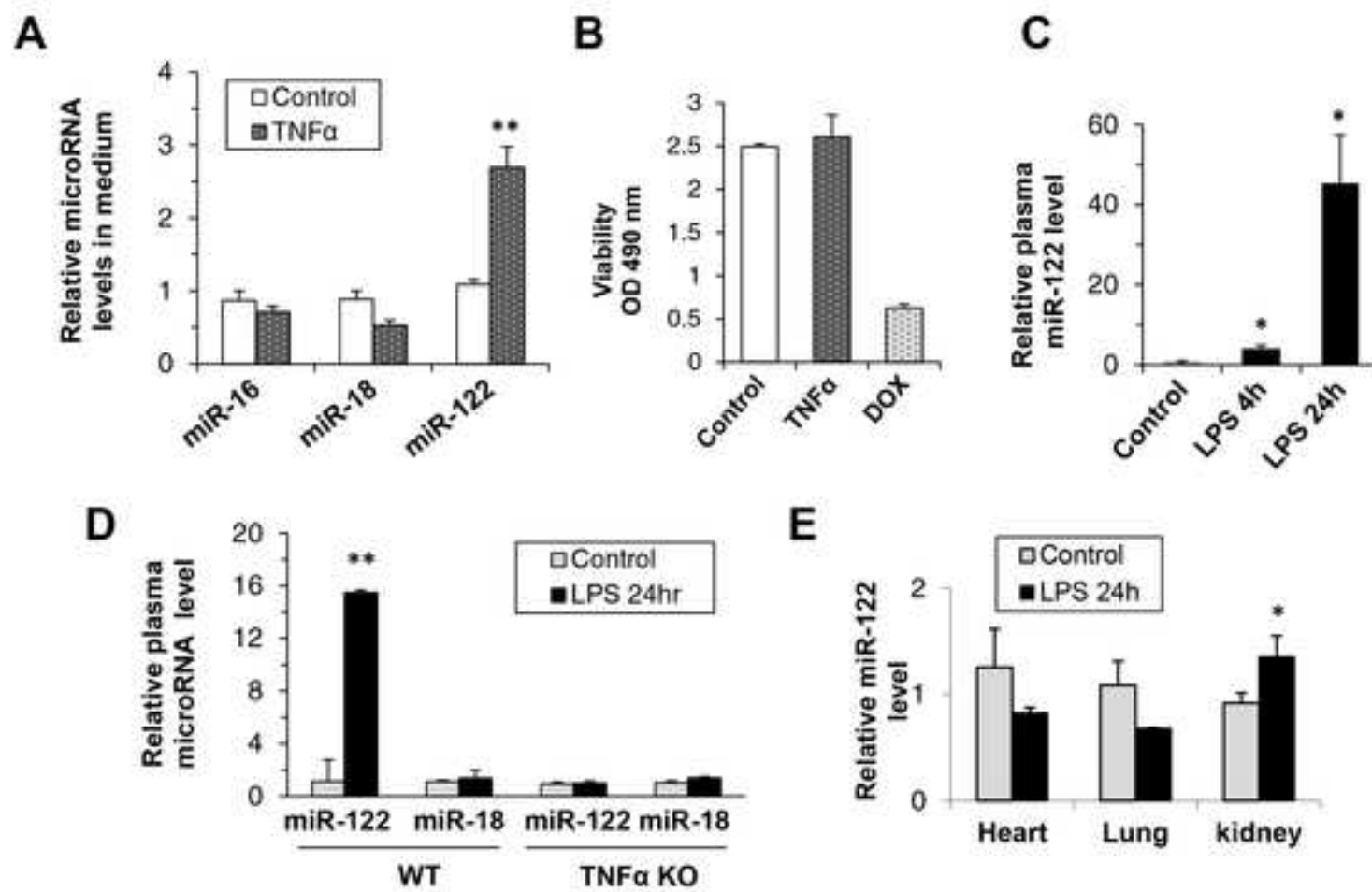


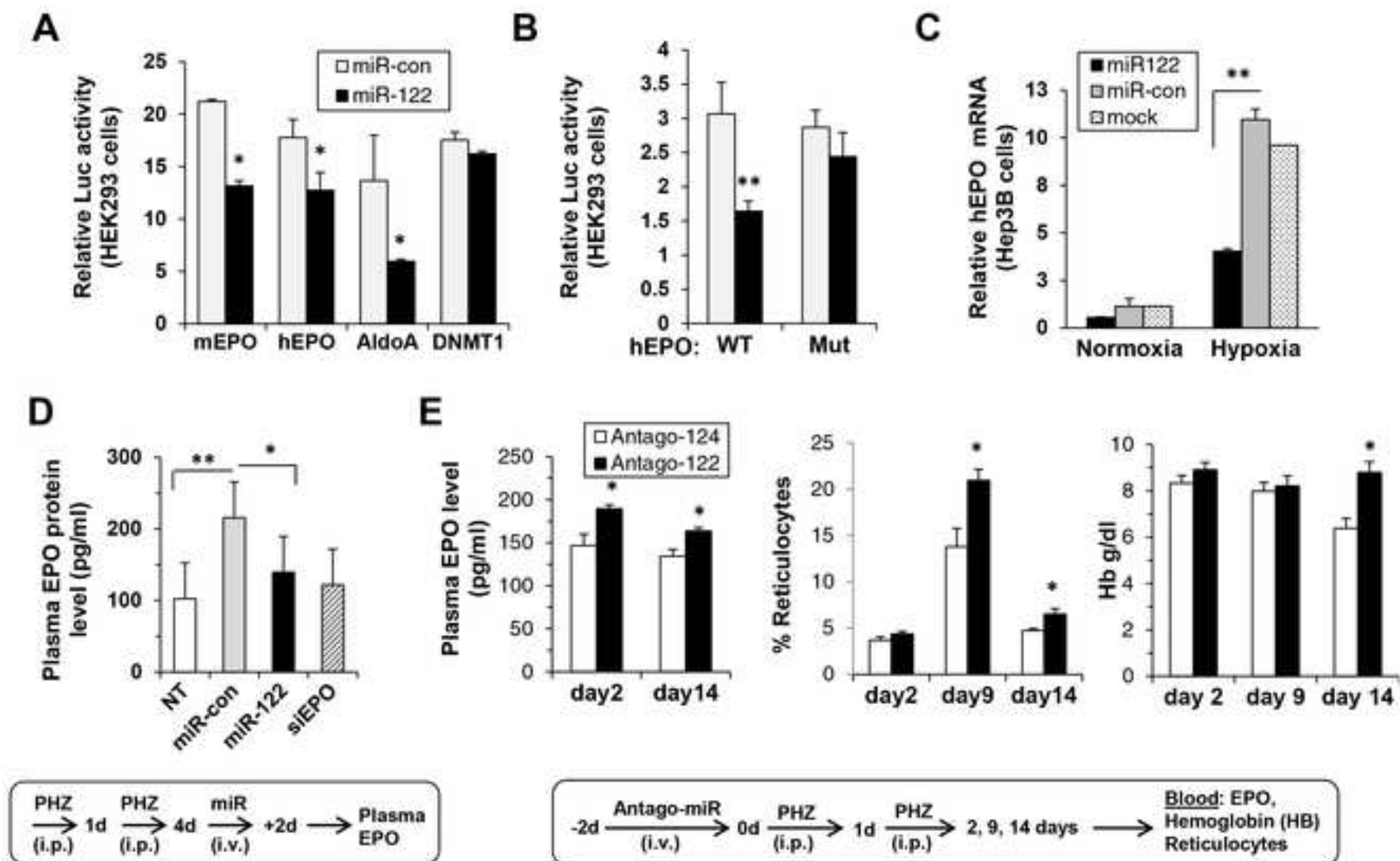
C

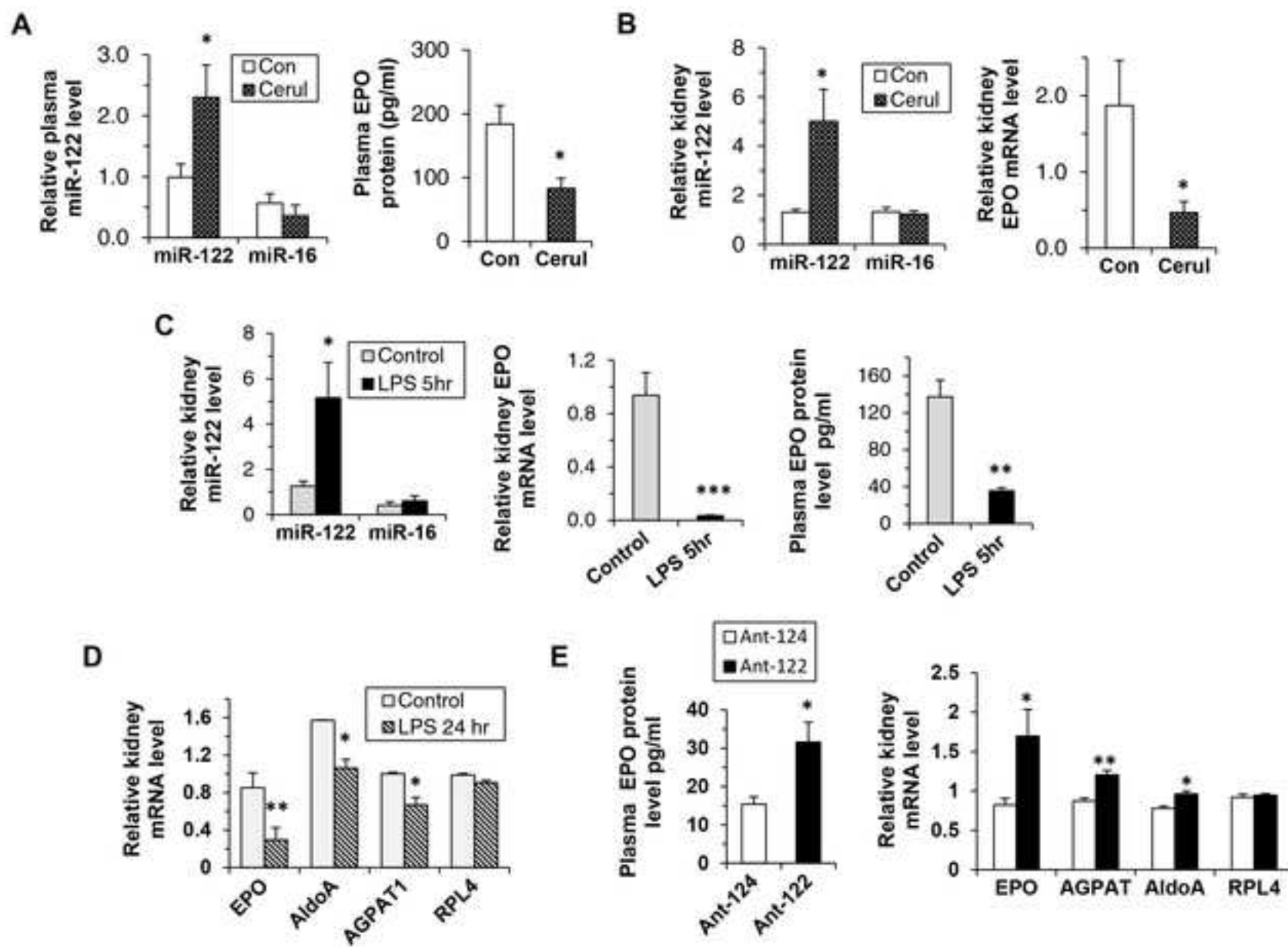


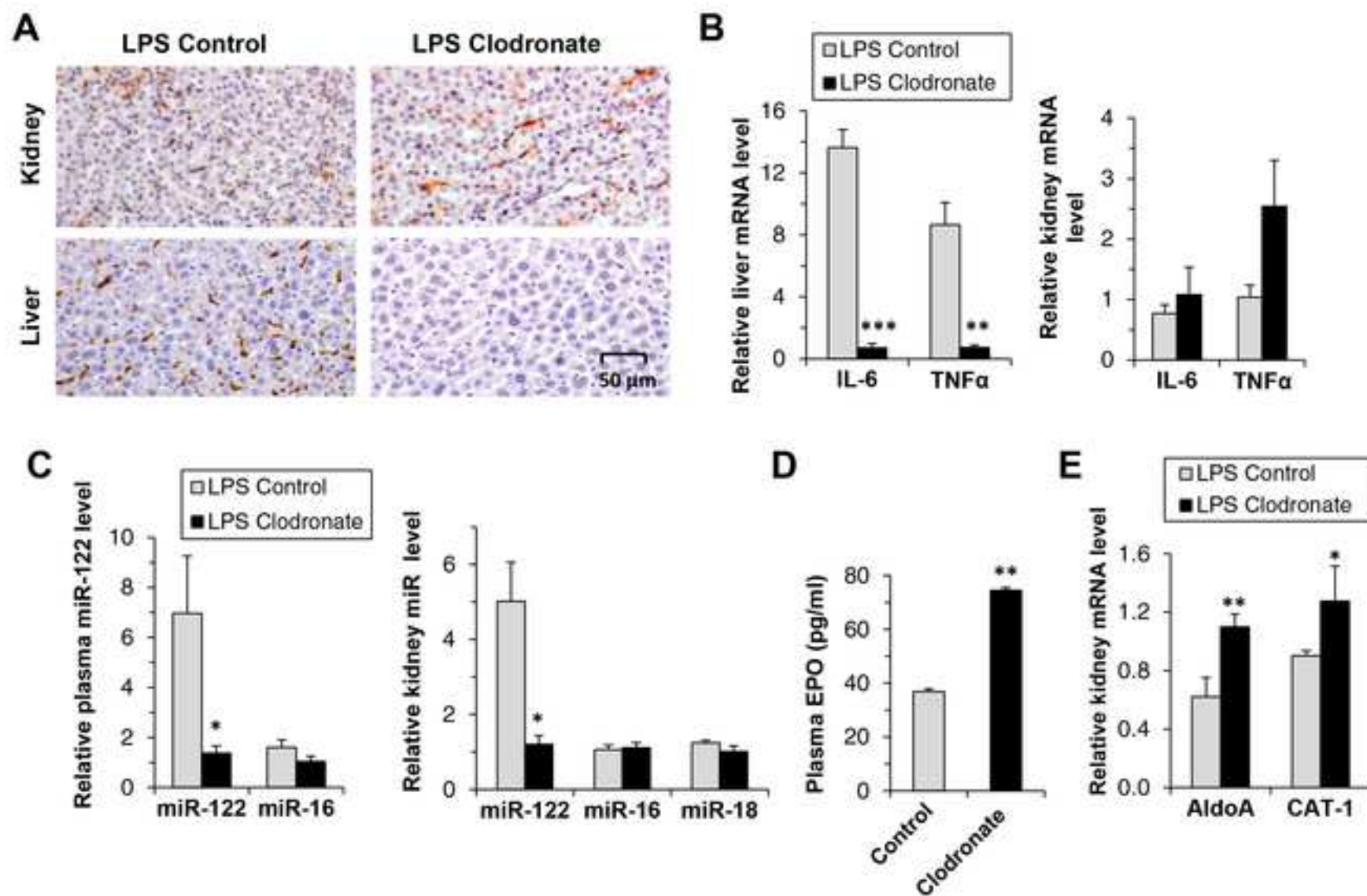
D

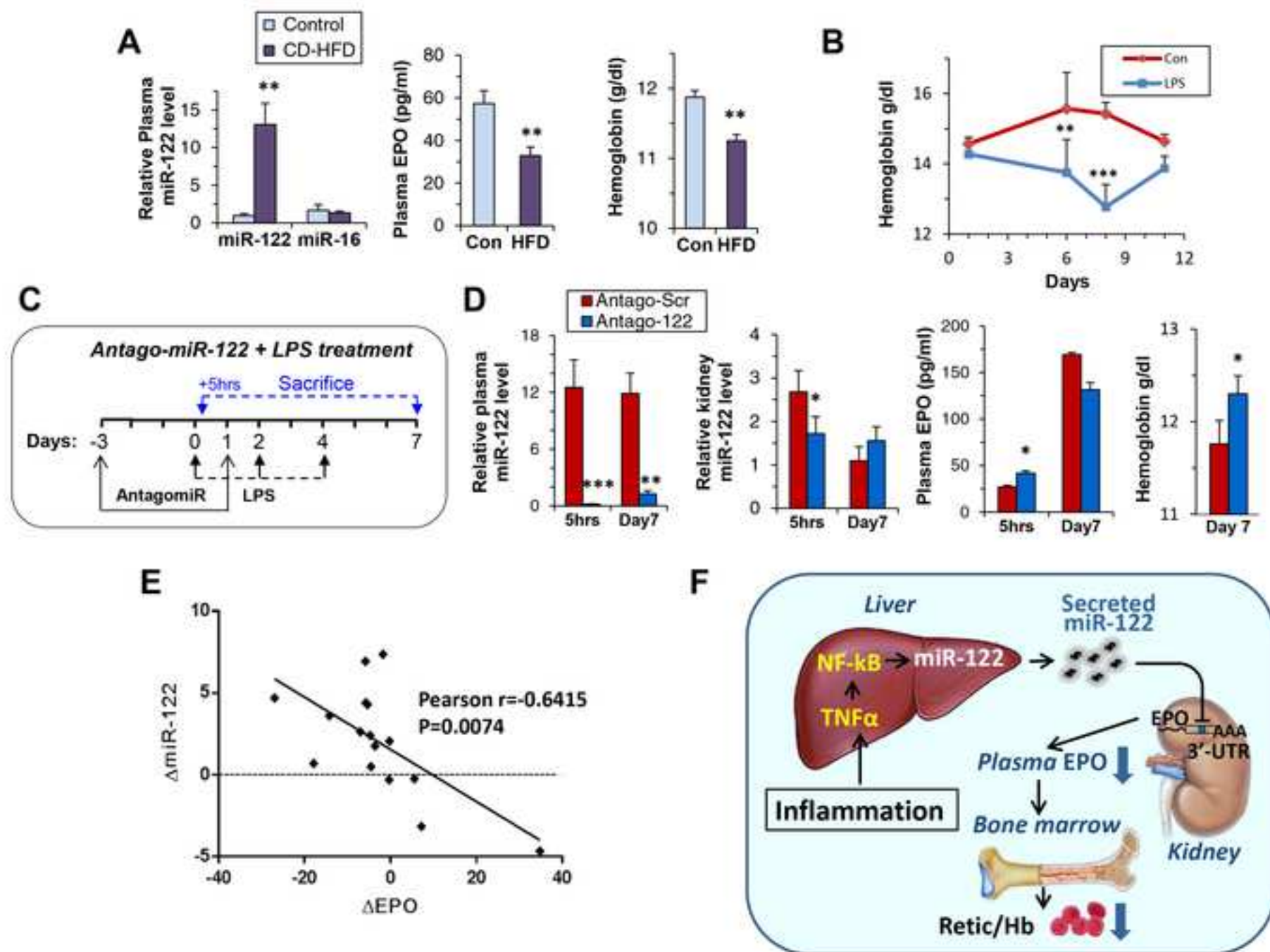












## Supplementary Materials and Methods

### *Plasmids*

The human miR-122 promoter fragments spanning the region from -900 or from -250 to +270 bp relative to the transcription start site (TSS) (plasmids PmiR-122-900 and PmiR-122-250) were generated by PCR on human liver DNA using primers P20-P21 and P22-P21 respectively and inserted into the PGL4 vector (Promega) upstream of the luciferase reporter gene (see Supplementary Figure 3 and Supplementary Table 3). Mutating the NF- $\kappa$ B site in the promoter region was performed by PCR using primers P23 and P24. The IL-8 promoter region was amplified by PCR on Huh7 genomic DNA using primers P25 and P26 and inserted into the KpnI/HindIII site of the PGL4 vector. The 3'-UTR region of the human (158 bp) and mouse (177 bp) EPO mRNA, containing two putative miR-122 target sites, were PCR amplified from human or mouse liver DNA using primers P27-P28-2 and P29-P30 respectively (see Supplementary Figure 9 and Supplementary Table 3). The PCR fragments were inserted into the pmirGLO vector (Promega) between the XhoI and Sall restriction sites, downstream of the firefly luciferase reporter gene. The 3'-UTR of human AldoA and the human DNMT1 mRNAs were PCR amplified using primers P31-P32 and P33-P34 respectively, and cloned in the pmirGLO vector between the SacI-XbaI sites. For construction of the miR-122 tester plasmid, primers P38-P39 were annealed and inserted between the SacI and XbaI sites of pmirGLO (see Supplementary Figure 3 and Supplementary Table 3).

### *Luciferase Assay*

For Luciferase assays, cells grown in 24 well plates were co-transfected with a luciferase reporter plasmid (50 ng) and 1 ng of *Renilla* Luciferase vector (PRL, Promega) using the TransIT-LT1 (Mirus) transfection reagent (MIR 2300, Madison, WI). In experiments where Luciferase reporter plasmids were transfected together with mimic-microRNA or antago-miRs, (50 nM) cell transfection was performed with Lipofectamine LTX (Invitrogen). *Firefly* and *Renilla* luciferase activity was assessed using the Dual Luciferase Reporter Assay system (Promega). Readings were taken in triplicates on a Mithras LB 940 Luminometer (Berthold Technologies).

### *Cell Proliferation Assay*

Cell proliferation assay was performed with the CellTiter 96 Aqueous One Solution cell proliferation assay (MTS) (Promega) on Huh7 cells seeded in 96-well plates and 24 hours later, cells were treated with TNF $\alpha$  (5ng/ml) for 24 hrs. Antitumour antibiotic Doxorubicin (DOX) 2 $\mu$ g/ml was used as a proliferation inhibitor control. After 24 hours, MTS solution was added (20  $\mu$ l/well), and cells were incubated for 3 hours at 37°C. The number of living cells in the culture was determined by absorbance at 490 nm with a 96-well plate reader. The data is presented as the mean  $\pm$  SD (n=3).

### *In Vivo Luciferase Activity Monitoring by the IVIS Camera*

For in vivo bioluminescence imaging, mice were hydrodynamic tail vein injected with 2 ml saline containing 5  $\mu$ g of the human PmiR-122-900 luciferase reporter plasmid. One day after injection, the animals were injected i.p. with 500  $\mu$ l of D-luciferin (Promega).

Ten minutes after luciferin injection, mice were imaged using an IVIS-200 CCD camera (IVIS-200; Xenogen, Alameda, CA). Immediately after imaging, mice were i.p. injected with LPS (1mg/kg mice) or with saline and imaged again 3 hours later and at days 1, 2, 5, 6 and 7 after LPS injection. Luciferase quantification was done using Living Image® software (Xenogen Corp.). *In vivo* luciferase activity is expressed as photons/second/cm<sup>2</sup>.

### *Induction of Anemia with Phenylhydrazin*

Anemia was induced with Phenylhydrazin (PHZ) (30 mg/kg body weight) (Sigma Chemical, St Louis, MO) by i.p. injection on 2 consecutive days in 200 ul saline. In the experiment with mimic-miR-122, four days after the second PHZ injection, mimic-miR-122, miR-control (siScrambled) or siEPO were i.v. injected (0.1 mg/mouse in 200ul saline) and 2 days later, blood was taken for measurement of EPO protein levels. In the experiment with repression of miR-122, mice were i.v. injected with antago-miR-122 or antago-miR-124 (negative control) (5 ug/mouse in 1.5ml saline) and the next day, blood was drawn for measurement of reticulocytes, hemoglobin and EPO levels. Mice were then i.p. injected with PHZ on 2 consecutive days and blood was taken at 7 and 12 days after the second PHZ injection for measurements of reticulocytes, hemoglobin and EPO levels.

### *Induction of Acute Pancreatitis by Cerulein*

C57BL/6 mice, 7-8 weeks old, were injected intra-peritoneally (i.p.) with 50 µg/kg Cerulein (C9026, Sigma-Aldrich) in 0.1 ml of saline, repeatedly every 1 h (a total of 6

injections). Saline was injected as control. Mice were sacrificed 1 hour after the last cerulein treatment.

### *Macrophage Depletion by Clodronate*

C57Bl/6 mice (7-8 weeks old) were injected i.p. with 200  $\mu$ l of clodronate liposomes or with phosphate-buffered saline (PBS) liposomes (purchased from clodronateliposomes.org), two days before LPS injection (1mg/kg). The rat antimouse F4/80 antigen (No. MCA497) was purchased from; AbD Serotec (ENCO ).

### *A Mouse NASH Model*

The mouse CD-HFD model, recapitulating key features of the human metabolic syndrome – Non-Alcoholic SteatoHepatitis (NASH), was induced by long-term feeding with a Choline-Deficient High-Fat Diet, developed by Heikenwalder et al. {Wolf, 2014 #81}. At the age of 12 months, these mice have a significant elevated TNF $\alpha$  serum levels. Blood was sampled at 12 months of age of these mice and measured for EPO protein and miR-122 levels.

### *RNA Extraction and Quantitative Real-Time PCR Analysis*

Total RNA, including small RNAs, were isolated from 200  $\mu$ l of plasma or culture media samples using the miRNeasy Mini kit (Qiagen, Valencia, CA,USA) with 2 minor modifications. First, 200  $\mu$ l of plasma or culture media were lysed with 1ml of Qiazol solution. Second, a 50 pmol/l of synthesized single strand *Caenorhabditis elegans*

miRNA (cel-miR-39) was added as the spike-in control to monitor extraction efficiency.

The remainder of the RNA extraction was performed according to the manufacturer's instructions. miRNAs were eluted with 30  $\mu$ l of RNase-free water.

Total RNA, including miRNAs, from cells or tissues were isolated using TRIzol reagent (Invitrogen, Carlsbad, CA, USA). cDNA was synthesized using the Quanta Biosciences qScript™ cDNA Synthesis Kit (95047-100) for mRNA analysis, and using the qScript™ microRNA cDNA Synthesis Kit (95107-100) for miRNAs analysis. qRT-PCR of miRNAs and mRNA was performed using the ABI 7900 HT Real-Time PCR System and a SYBR Green PCR Kit: Quanta Cat. #84018 and #84071 respectively. The fold expression and statistical significance were calculated using the  $2^{-\Delta\Delta C_t}$  method. All experiments were performed in triplicates. The primers used for qPCR are shown in Supplementary Table 2.

### *Synthetic small RNA*

Small RNA duplexes were purchased from Syntezza Bioscience Ltd (Israel). The microRNA inhibitors: Antago-miR-122 and antago-miR-124, were purchased from Sigma Aldrich (Israel).

**Mimic-miR-122:** sense: 5' -CAAACACCAUUGUCACACUCCATT-3'

antisense: 3' - TTGUUUGUGGUAACAGUGUGAGGU-5'

**Modified miR-122:** sense: 5' -mCmAAACACCAUUGUmCACACUCmCmA dT dT-3'

antisense: 5' -mUmGGAGUGUGACAAUGGUGUUmUG dT dT-3'

**siEPO (modified):** sense: 5' -mGACCCUmUCAGCUUCAUAmUmA dT dT-

3' antisense: 5' -mUAUAUGAAGCUGAAGGmGmUC dT dT-3'

si-Scrambled :sense: 5'-GmUmUGGAGmGCGGUAmUGUGmAGdTdT-3'

antisense: 5'-CmUmCACAUACCGCCUCCmAmACdTdT-3'

### *Northern Blot Analysis*

Total RNA (40 µg) from human liver or Huh7 cells was separated on a 1.2% formaldehyde agarose gel and transferred onto GeneScreen Plus® Hybridization Transfer Membrane. For RNA size determination we used the RNA Millenium Size Markers-Formamide (Ambion, Cat. # 7151). Radioactive  $\alpha$ -<sup>32</sup>P-dCTP labelling of the probes was carried out using Random Primer DNA Labeling Mix (Biological Industries, Beth Haemek, Israel). Membranes were hybridized with ExpressHyb-Hybridization Solution (Clontech).

### *mRNA 3' RACE Analysis*

RNA was extracted from Huh7 cells using the TRIzol reagent (Invitrogen) and subjected to 3'-RACE analysis using the GeneRacer kit (Invitrogen). cDNA was generated with primer P5 followed by a first PCR amplification using the pri-miR-122 specific forward primer P11, and the GeneRacer 3' primer (P10). A second PCR was performed on the first PCR reaction using nested pri-miR-122 primer, P13, and the GeneRacer 3' Nested Primer, P12 (Figure 1). The amplified 3'RACE fragment from the second PCR, was purified and sent for sequence analysis (Supplementary Figure1). See Supplementary Table 1 for primer sequences.

### *Human Blood Samples*

For analysis of blood samples collected from patients with inflammation, we submitted and received an IRB approvals for the collection of blood samples for the measurement of miR-122 and EPO both from the Hamburg-Eppendorf University Hospital and Hadassah Hebrew University Hospital. The samples received from Hamburg-Eppendorf University Hospital were obtained from the “Liver.net” biobank, which was established by the Collaborative Research Centre 841 at Hamburg University Medical Center.

### *Hematological Blood Parameters*

Blood from the retro-orbital plexus was collected into microcapillaries. The hemoglobin content was analyzed by Reflotron Hemoglobin test (REF 10744964, Roche diagnostic). Reticulocyte numbers were measured using the COULTER® LH780 Hematology Analyzer (Beckman Coulter, Inc., CA, USA) and EPO plasma levels were determined by mouse EPO Quantikine ELISA kit (MEP00B, R&D Systems).

### *Immunofluorescence staining*

Liver tissue was cut into 5 mm sections, deparaffinized with xylene and hydrated through graded ethanol. For GFP (ab6673, Abcam) staining, a 25mM citrate buffer pH 6.0 was used for antigen retrieval, cooked in a pressure cooker for 20 min and left to cool for 30 min at room temperature. Slides were washed in Optimax (Pharmatrade) and incubated with primary antibody (diluted in CAS-Block (Zymed) 1:250, over night at 4<sup>o</sup>C. Sections were rinsed in PBS and incubated with 488-conjugated donkey anti- goat immunoglobulin G (Jackson ImmunoResearch Laboratories). Sections were washed

twice in PBS for 5 min, in ddH<sub>2</sub>O twice for 5 min, and were mounted with fluorescent mounting media.

### *Chromatin Immunoprecipitation (ChIP)*

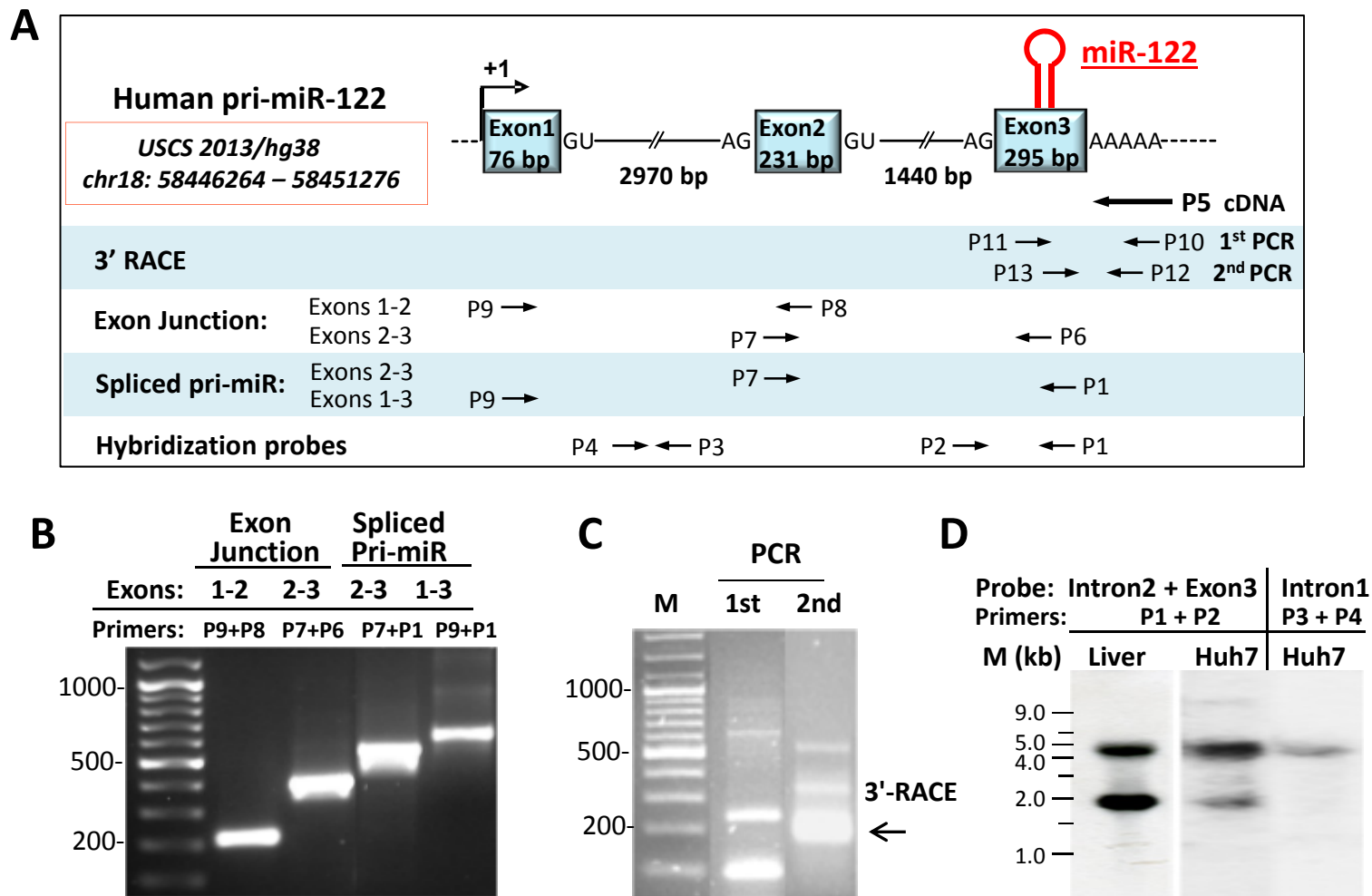
ChIP assay was performed as described in Rubins et al., (2005) *Molecular and Cell Biology*, Vol. 25:7069-77, and in Jun Yang et al., (2015) *Mol Cell Proteomics*, Vol.14(10):2701-21. Briefly, Huh7 cells ( $1 \times 10^7$ ) were treated with TNF $\alpha$  (5ng/ml) for 2 or 16 hrs. Cells were then fixed with 1% formaldehyde, lysed and the chromatin was sheared by sonication for 15 minutes. The chromatin was then immunoprecipitated using the Anti-p65 Antibody (ab7970 abcam). Real-time PCR was performed to quantify the relative enrichment of immunoprecipitated DNA. The relevant primers are listed in Supplementary Table 2. The enrichment of target genes was calculated using the GAPDH as a reference for nonspecific DNA, and is shown relative to the input Chromatin.

### *Statistical Analyses*

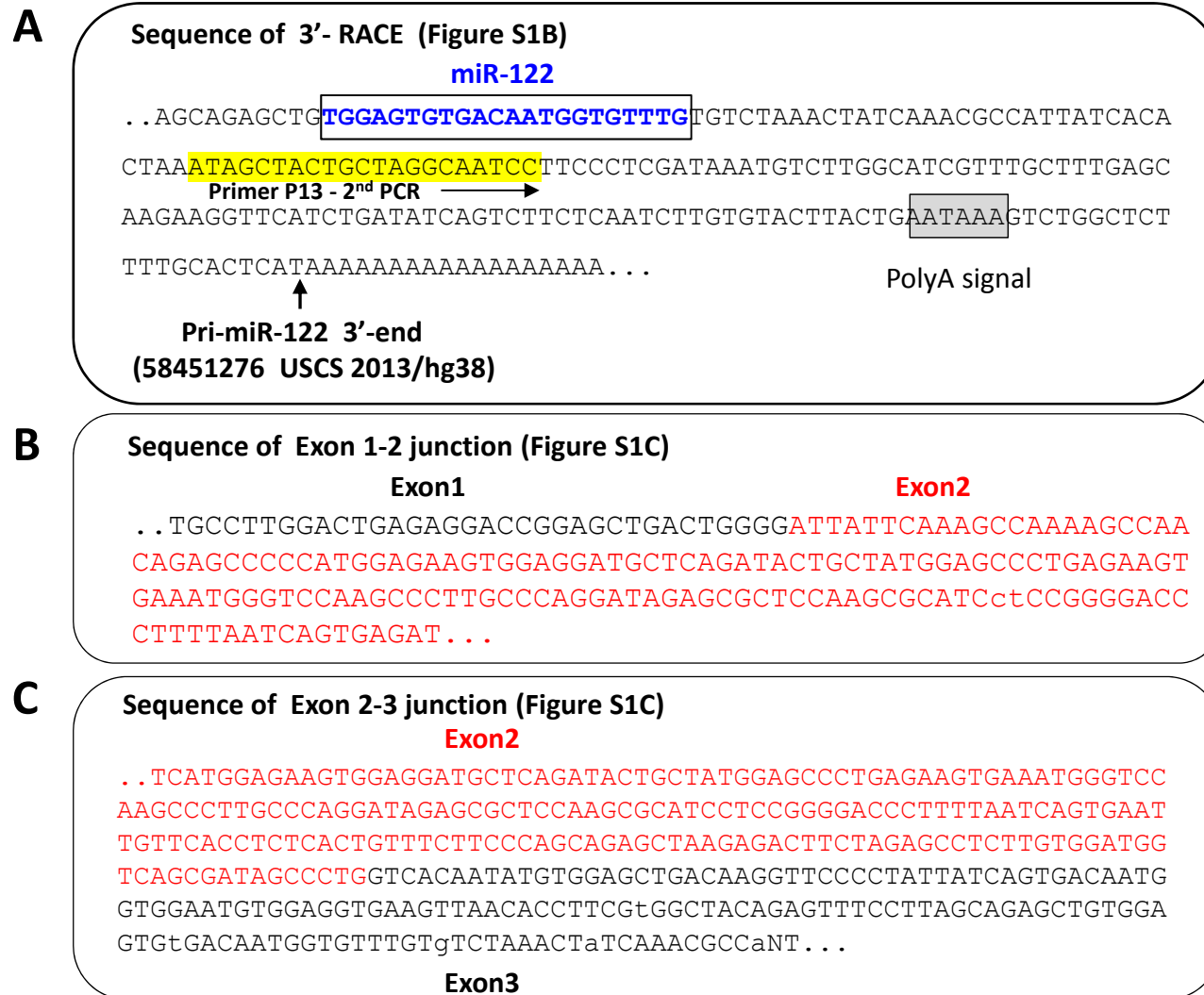
All data were subjected to statistical analysis using the Excel software package (Microsoft) or GraphPad Prism6 (GraphPad Software Inc., La Jolla, CA, USA). Two-tailed Student's t- tests and Pearson's correlation coefficients were used to determine the difference between the groups. Data are given as mean  $\pm$  SD, and are shown as error bars for all experiments. Differences were considered significant at  $P < 0.05$ . To determine group sizes necessary for adequate statistical power, power analysis was performed using preliminary data sets. The exclusion criterion was set to be 1.5 s.d. from the mean. No data met this criterion, and thus all data points were included in the

analysis. The investigators were blinded to group allocation during collection and analysis of the data.

ACCEPTED MANUSCRIPT



**Supplementary Figure 1. miR-122 is generated from the third exon of a 5 kb pri-miR-122 transcript carrying three exons. (A)** A schematic presentation of pri-miR-122 with the sizes of the 3 exons and the introns and its coordinates in the UCSC 2013/hg38 assembly, and the primers used for the analysis (see primer sequences in Supplementary Table 1). **(B)** cDNA generated by RT-PCR on Huh7 RNA using primer 5, followed by PCR to identify the spliced RNA structure. **(C)** PCR reactions to identify the pri-miR-122 3'-end using a 3'-RACE kit (invitrogen). All PCR products were sequenced (see Supplementary Figure 2). **(D)** Northern blots were probed with PCR fragments carrying the Intron2-Exon3 region or a region of intron1, generated by the indicated primers (1+2 and 3+4 respectively, Table S1). This analysis yielded two prominent bands, one 5.0 kb (corresponding to full pri-miR-122), and 2.0 kb. The small Pre- and mature miR-122 RNA run-off these gels. The 2.0 kb fragment yielded a signal with mature miR-122, but not with a probe carrying only intron1 sequences, indicating that it is a partially spliced product lacking intron1.



**Supplementary Figure 2. Determination of the pri-miR-122 structure and its 3'-end.** Sequencing results of products of RT-PCR reactions performed on cDNA obtained with primer P5 (Supplementary Figure 1). **(A)** Sequencing of 2<sup>nd</sup> PCR product of the 3'-RACE analysis generated with primers P13 and P12. The terminal nucleotide at position 58451276 is annotated. Mature miR-122 sequence is shown in blue, the position of primer P13 is shown in yellow and the polyA signal sequence is shown in gray. **(B)** DNA sequencing of the PCR product generated with primers P9 and P8 (Exon 1-2 junction). **(C)** Sequencing of PCR product generated with primers P7 and P6 (Exon 2-3 junction). The DNA sequence of Exon2 is shown in red.

A

**P20 (-900)**

...GAGGATCACCTGAGGTCAGGAGTTTGGGACCAGCCT **AGTCAACATGGTGAAACCC**CGTCTCTACTAAAAATACAAAAATTAG  
 CCGGGCGTGGTGGCGGGCACCTGTAGTCCCAGCTACCCAGGAGGCTGAGGCAGGAGAATCGCTTGAATCCGGGAGGCGGAGGT  
 TGCAGTGAGCCAAGATCACGCCACTGCACTCCAGCCCAGGCAACTGAGCGAGACTCCATTTCAAAAAATAAGTAAATAAAAA  
 AAAAAAGCAATAATAATAGCCGACAACAGAATACAGCTAGGCCGAGCAGCAGCCTCCTCTGCTGTCCGTGCGGCTCGCCTGT  
 TGCCTGCTTCACTGCCTGACTGTGGGCTCTGTTTGTCTTGGTCCCCGTGGCATTACCAGAGCTTAGCAGATAAGGAGGAGCTT  
 CATAATAATTGTTGGCGTGAACAAAGGAATGCATGGTTAACTACGTGAGAAATGACCAGTTCAAGAGGAGAATGAGATTGGC  
 TTCCAAATGTTGGTCAAGAGCTCTACGTAGCATGAGCCAAGGATCTATTGAACTTAGTAGGCTCCTGTGACCGGTGACTCTTC  
 TGTCTCTAGAAATCTGGGGAGGTGACCAGGTGACATGCGAGTCTTCCCCTGAGGAACGTTAACTGGTTGGAAGTTGGGGT

**P22 (-250)**

TCTGAGGGGAAGATGTATTCACTAGGT **GACCTGTCTTCTCTGCCTCGG**TGGCCTCCATGGCTGCCTGCTGGCCGCACACCCCC

**NF-kB**

ACTCAGCAGAGGAA **TGGACTTTCC**AACTCTTGCTGAGTGTGTTTGACCAAAGGTGGTGTGACTTAGTGGCCTAAGGTCGTGCC  
 CTCCCTCCCCACTGAATCGATAAATAATGCGACTTATCAGAAAGAGAAAGAATTGTTTACTTTTAAACCCTGGATCCCATAA

→ **TSS** **Exon1**

AGGGAGAGGGGAGAGGCCTAAAGCCACAGAAGCTGTGGAAGGCGCCATCCTGCCTGCCACAGGAAGGGCCTTGGACTGAGAGG  
 ACCGGAGCTGACTGGGGGTAAGTGC GGCTCTCCCCGGCGCCTGCCGACCCCCCTGAGTGATCAGGCCGTTCTTTGGGGTGGC  
 CGCTGACCGAGAAATGACGGGAGGCTGCTGACTCCGGTGTGAAAAGATGCCACCCAGCGCCTGAGCAACAGGAGGTGTTGA

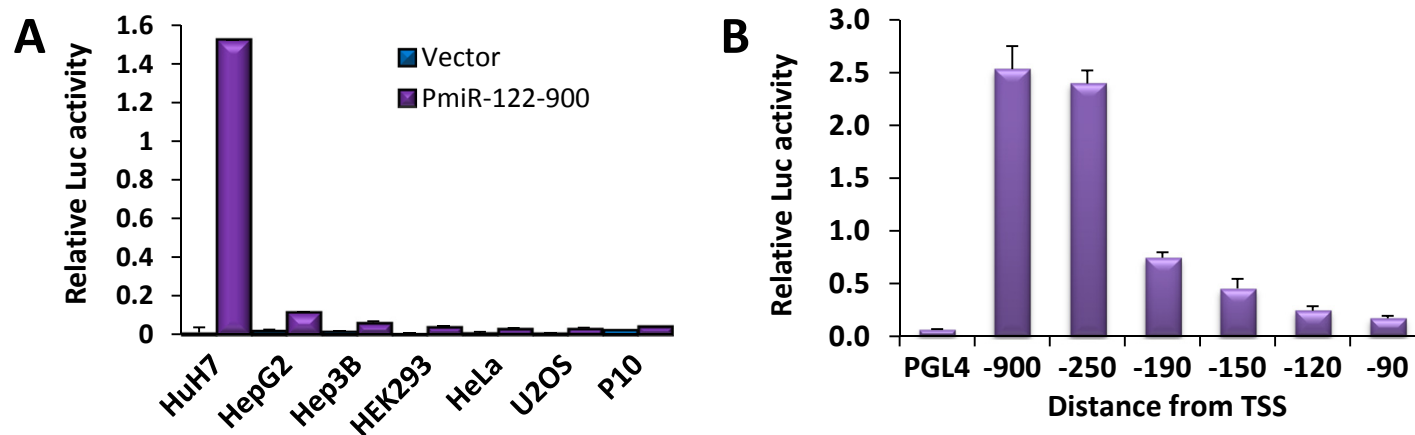
**HindIII (+270)**

ACACACCATAACTTTGTCTTCCATGATTATTCTGTTTCCCTCAGAA **AAGCTT**GAGGAAAAGTGGAGACTTTCTTTAGAGAGAGTA  
 ACAGATGGTTTCCGTTTAAAGAAAAATAACAAAATGGCTTAAAGGAGGAAAAGAAATGATCACCCCTGCAGAGGGAGAGAGGATG  
 AGGCTGGGGAGGAGCTGAGGGCTCAGGGACGGTGTGGGGTTTTATTTCTGCCCTTGGAGTGGCTGGACATTAAGCCAGTTCTT  
 GTTTTTACGATGGCCTGATTCAGCAATAACACCAAACCTTCAAACAAAATGCCGGCATTAGAGTCGTT **CCTTTGGCATGCCTC**  
**TGTCCAGG**TCATATTGTTCCCTCAATAGCACTAAAAATAGCTGGACACCTGTGCA.. **P21**

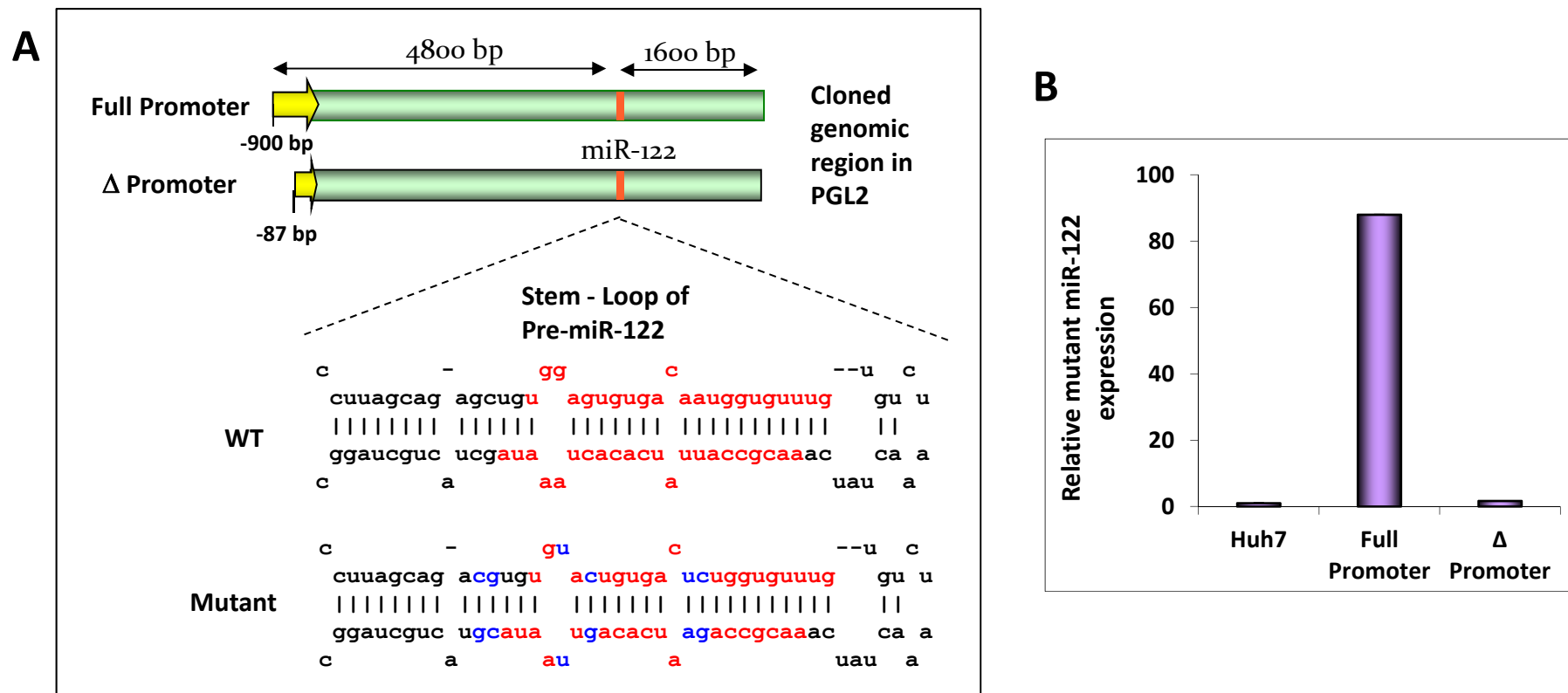
B

<b>SacI</b>	<b>XbaI</b>
5' - CCAAACACCATTGTCACACTCCAT -3'	
3' - TCGAGGTTTGTGGTAACAGTGTGAGGTAGATC -5'	

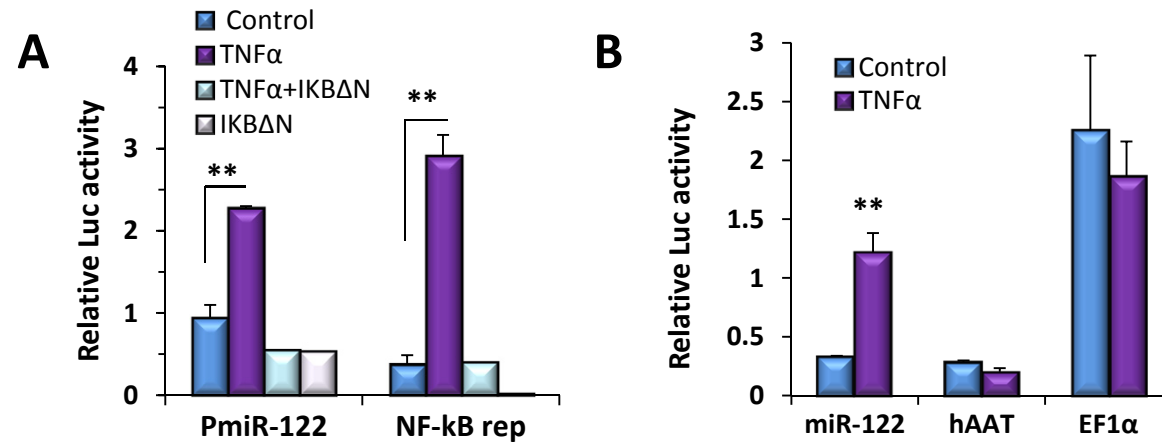
**Supplementary Figure 3. DNA sequence of the miR-122 promoter region.** (A) The miR-122 promoter region, extending to -900 or to -250 bp from the transcription start site (TSS) was amplified by PCR on human liver DNA, using primers P20 and P21 or P22 and P21 respectively (yellow). PCR products were digested with HindIII (light blue) and MluI (added to the 5'-end of primers P20 and P22, see supplementary Table 3), and cloned into the PGL4 vector, yielding plasmids PmiR-122-900 and PmiR-122-250 respectively. The NF-kB site at position -170 from TSS is marked in green. The cloned promoter region extends to +270 bp and includes Exon 1 (marked in grey). (B) Primers used for construction of the miR-122 tester plasmid in pmirGLO.



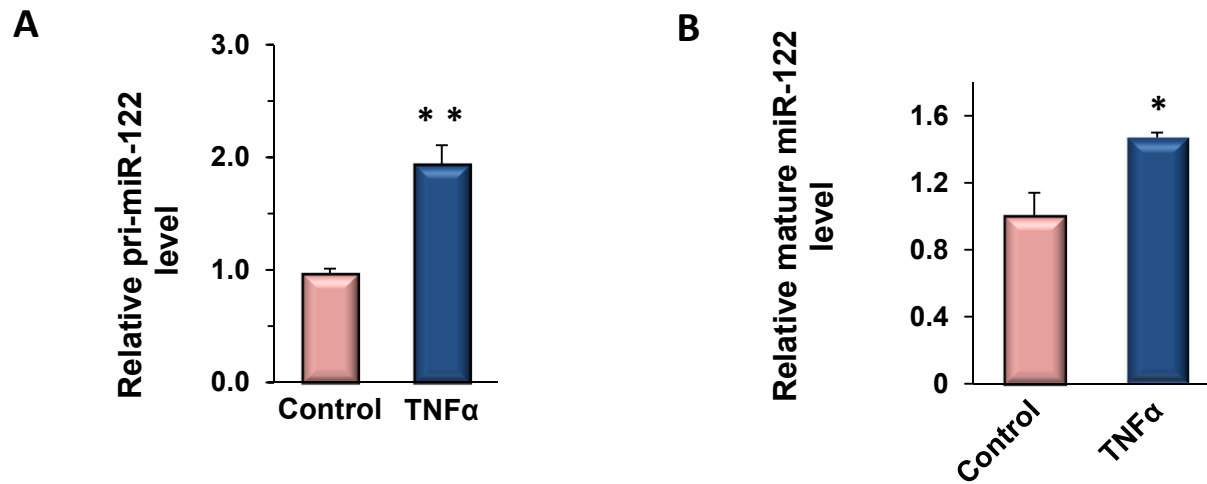
**Supplementary Figure 4. Analysis of miR-122 promoter activity.** (A) Expression of the miR-122 promoter in different cell lines. Cells were grown in a 24 well plate and transfected with plasmid PmiR-122-900 (50 ng). (B) Serial shortening of the miR-122 promoter from the 5'-end performed by PCR on DNA of the PmiR-122-900 plasmid, using forward primers corresponding to the sequence at the indicated distance from TSS (carrying an MluI or KpnI site at their 5'-end, Supplementary Table 3) and a reverse primer from the vector. The PCR fragments were digested with MluI or KpnI and HindIII (located at the 3'-end of the original promoter fragment, +270 from TSS) and inserted into the PGL4 vector. The plasmids (50 ng) were then used to transfect Huh7 cells grown in 24 well plates. Luciferase (Luc) activity was measured 48 hours after transfection and normalized to Renilla Luciferase activity expressed from a co-transfected pRL plasmid. Error bars = SD.



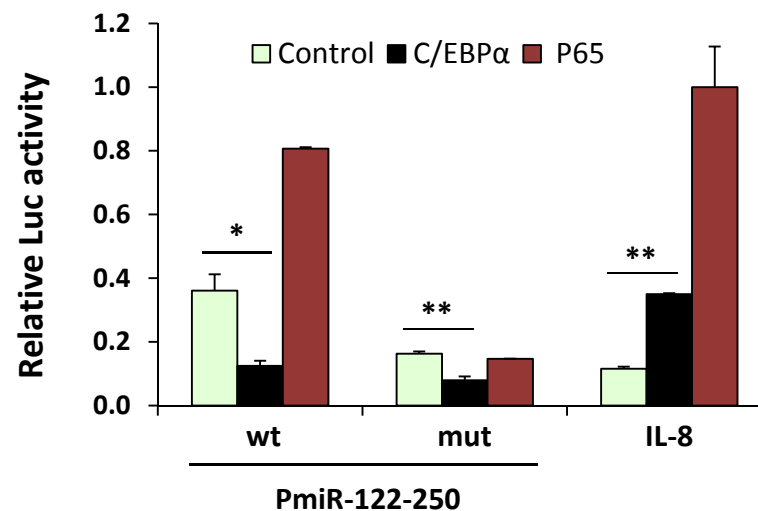
**Supplementary Figure 5. Mature miR-122 is generated solely from the long pri-miR-122 transcript driven by the upstream promoter. Rational:** Since the miR-122 promoter is expressed only in Huh7 cells, we exchanged the WT pre-miR-122 sequence within a plasmid carrying the entire miR-122 genomic region, with a mutated pre-miR-122, in order to distinguish its expression from the endogenous WT miR-122 of Huh7 cells. **Experimental design:** (A) Huh7 cells (that express endogenous miR-122) were transduced with plasmids harboring the mutated miR-122 genomic region, cloned with (full) or without ( $\Delta$ ) the promoter region. (B) 48 hours after transfection, RNA was extracted for qRT-PCR analysis of the mutant miR-122 (using a specific miR-122 mutant primer) which was normalized to RNU-43. **Results:** Deletion of the upstream promoter region abolished miR-122 expression, indicating that it is the only driver of the miR-122 transcript.



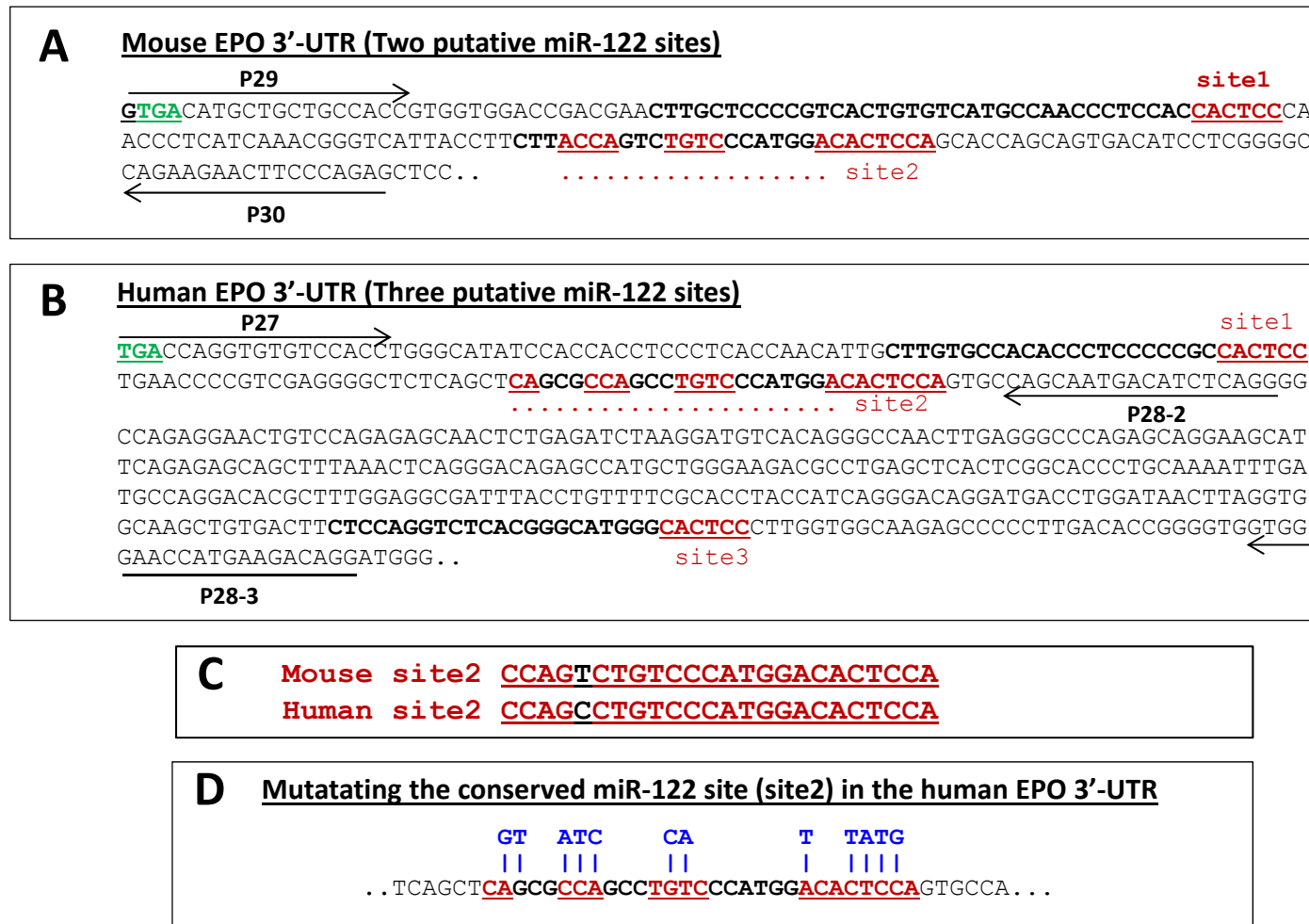
**Supplementary Figure 6. Activation of the miR-122 promoter by TNF $\alpha$  is specific and is NF- $\kappa$ B-dependent.** (A) Huh7 cells were co-transfected with 50 ng of PmiR-122-250 or the NF- $\kappa$ B reporter plasmid, together with a plasmid expressing the IKB $\Delta$ N inhibitor (50 ng), a dominant-negative NF- $\kappa$ B inhibitor which remains attached to NF- $\kappa$ B and does not release it to enable NF- $\kappa$ B activity. (B) Cells transfected with reporter plasmids for PmiR-122-250 and the human AAT and EF1 $\alpha$  promoters (which served as negative controls) and 24 hours later, treated with TNF $\alpha$  (5 ng/ml) for 24 hours. Luciferase (Luc) activity was measured 48 hours after transfection and normalized to Renilla Luciferase activity expressed from a co-transfected pRL plasmid. Error bars = SD. \*P < 0.05; \*\*P < 0.01.



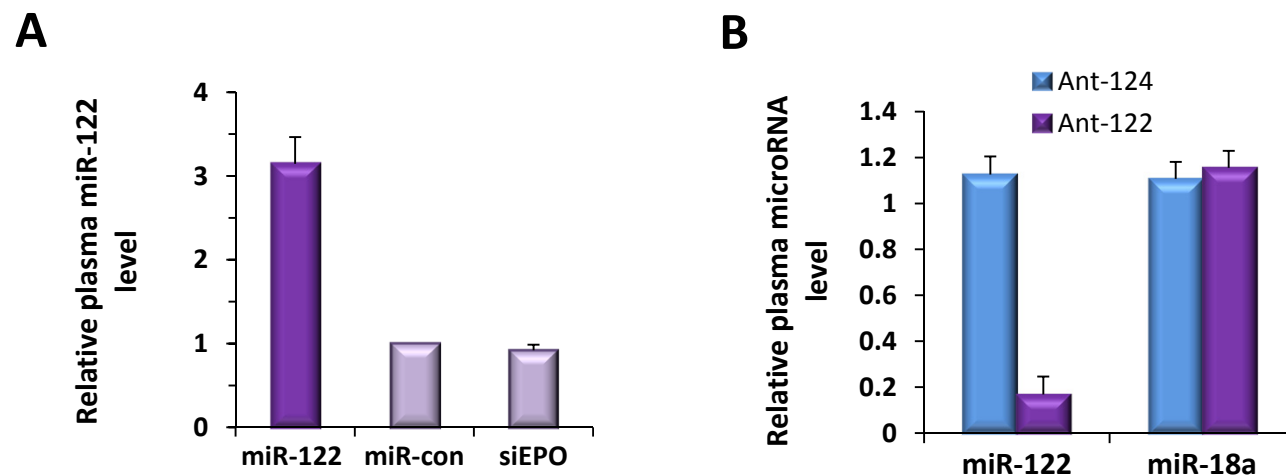
**Supplementary Figure 7. TNF $\alpha$  enhances both, pri-miR-122 and mature miR-122 levels in Huh7 cells.** qRT-PCR analysis of pri-miR-122 (A) and mature miR-122 (B) in RNA extracted from Huh7 cells treated with TNF $\alpha$  for 24 hours. Mature miR-122 was normalized to RNU-6, pri-miR-122 levels were normalized to HPRT. Error bars = SD. \*P < 0.05; \*\*P < 0.01.



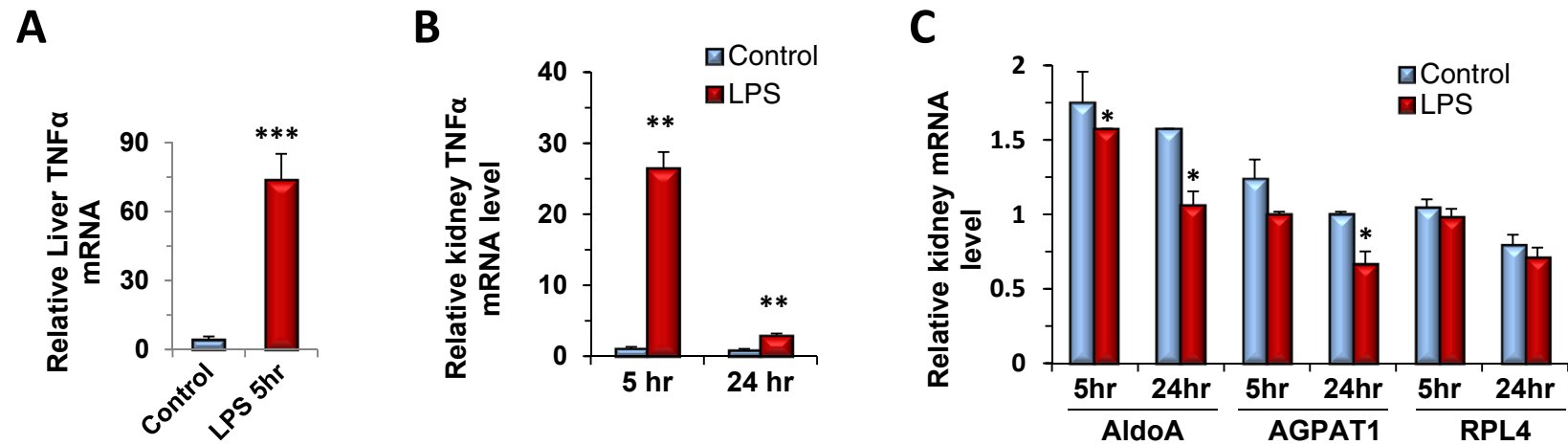
**Supplementary figure 8. C/EBP $\alpha$  represses the wt and the mutant miR-122 promoter.** Relative Luciferase activity in Huh7 cells, plated in a 24 well plate, co-transfected with 50 ng of wild type (wt) or mutant (mut) PmiR-122-250 plasmids or with an IL-8 reporter plasmids as a positive control (known to be activated by both, C/EBP $\alpha$  and NF-kB), together with a plasmid expressing P65 (25 ng), or the human C/EBP $\alpha$  (50 ng). Luciferase activity was measured 48 hours post transfection and normalized to Renilla Luciferase activity expressed from a co-transfected pRL plasmid. Error bars = SD. \*P < 0.05; \*\*P < 0.01



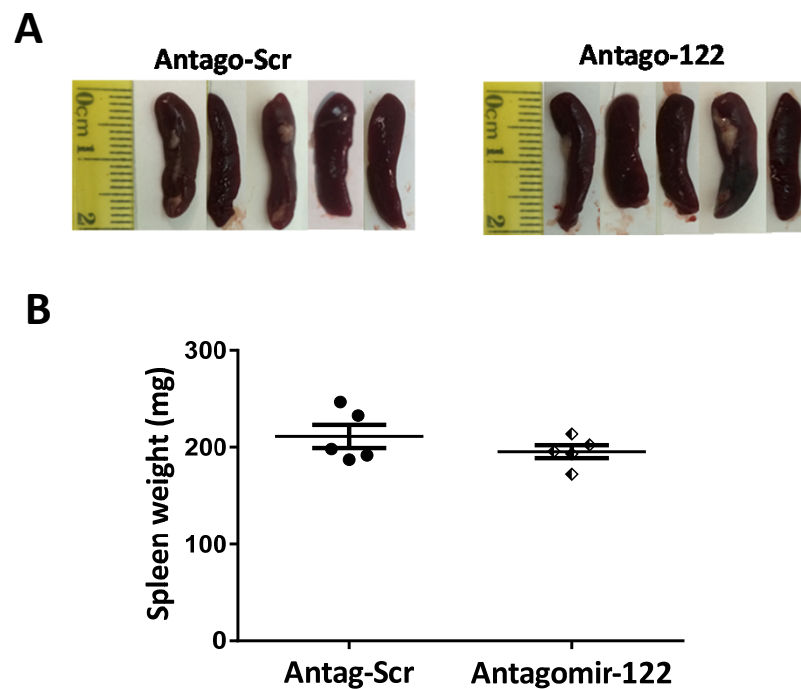
**Supplementary Figure 9. Putative miR-122 target sites in the 3'-UTR of erythropoietin (EPO).** (A and B) The sequence of the mouse and human EPO 3'-UTR region containing the putative miR-122 target sites. The miR-122 seed target and additional potential miR-122 binding sites are shown in red. The TGA translational stop codon of EPO is shown in green. The position of primers used for cloning the 3'-UTR into the pmirGLO plasmid are shown with an arrow. Complete primer sequences are shown in Supplementary Table 3. (C) Site2 is highly conserved between mouse and human EPO. (D) Mutations (shown in blue) that were introduced into the putative miR-122 site2 in the human EPO 3'-UTR.



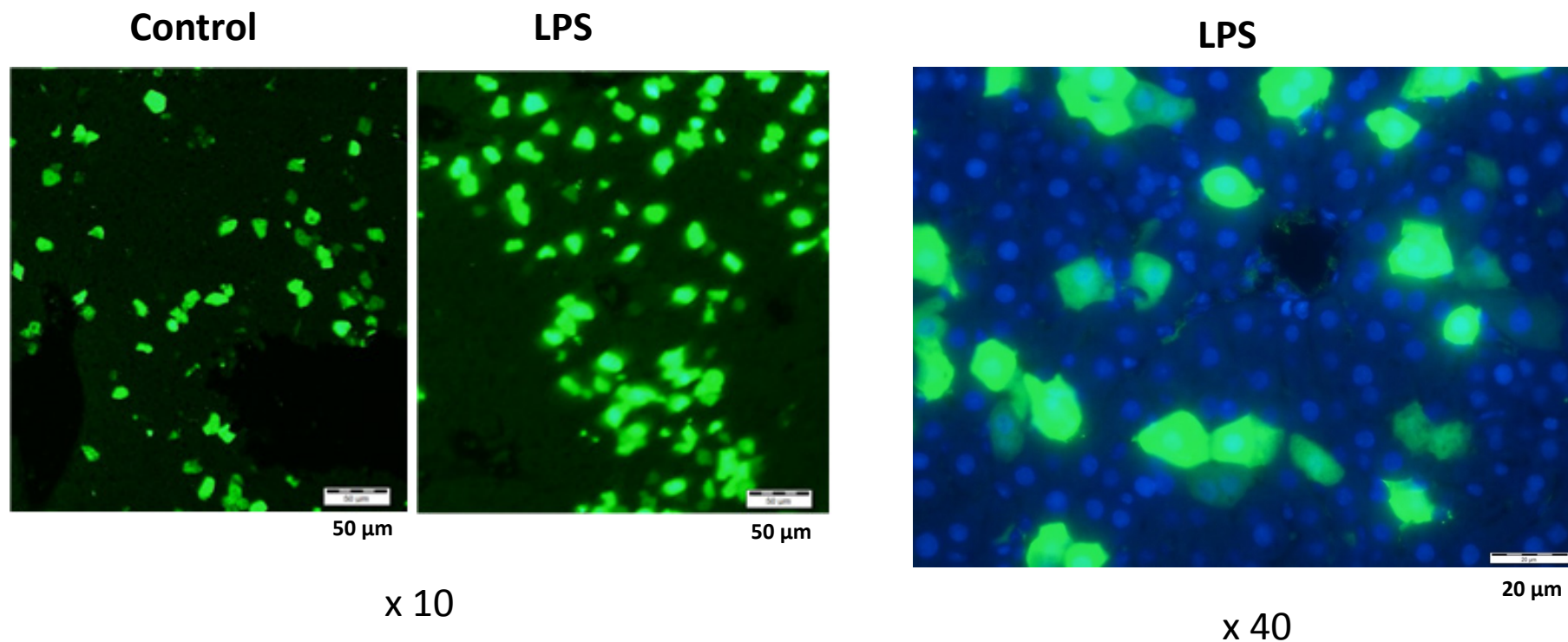
**Supplementary Figure 10.** (A) Blood microRNA levels in PHZ treated mice. Mice were injected i.p. in two successive days with PHZ (30 mg/kg) and 4 days after the second PHZ injection, mice were injected i.v. with mimic miR-122, miR-scrambled (miR-con), or siEPO (0.1mg/mouse) (modified for stability, see Materials and Methods). (B) The effect of antagomiR-122 on plasma miR-122 levels. C57BL/6 mice were injected i.v. with antagomiR-122 (5 $\mu$ g/mouse) (Ant-122) or antagomiR-124 (Ant-124) and 24 hours later miR-122 plasma levels were determined. miR-18a served as a negative control. MicroRNA plasma levels were measured two days after injection by qRT-PCR and normalized to spiked-in *C.elegans* miR-39 (Cel miR-39) (n=4).



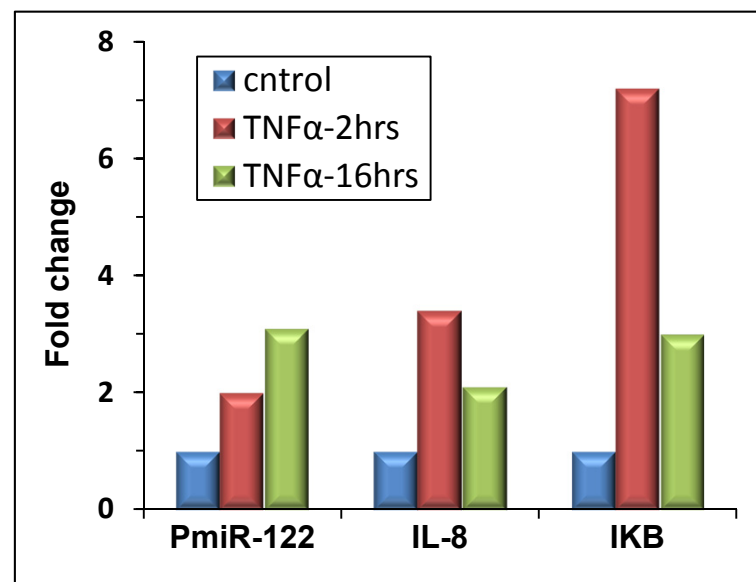
**Supplementary Figure 11. The effect of LPS on mRNA levels of TNF $\alpha$  and miR-122 target genes in the kidney.** C57BL/6 mice were injected i.p. with LPS (1mg/kg) and were sacrificed 5 and 24 hours later and RNA extracted from the liver and kidneys for qRT-PCR analysis of TNF $\alpha$  (**A** and **B**) and the miR-122 target genes AldoA and AGPAT1 (**C**). RPL4 served as a negative control. Kidney TNF $\alpha$ , AldoA, AGPAT1 and EPO mRNA levels were normalized to HPRT. Error bars = SD. \*P < 0.05; \*\*P < 0.01; \*\*\*P < 0.001.



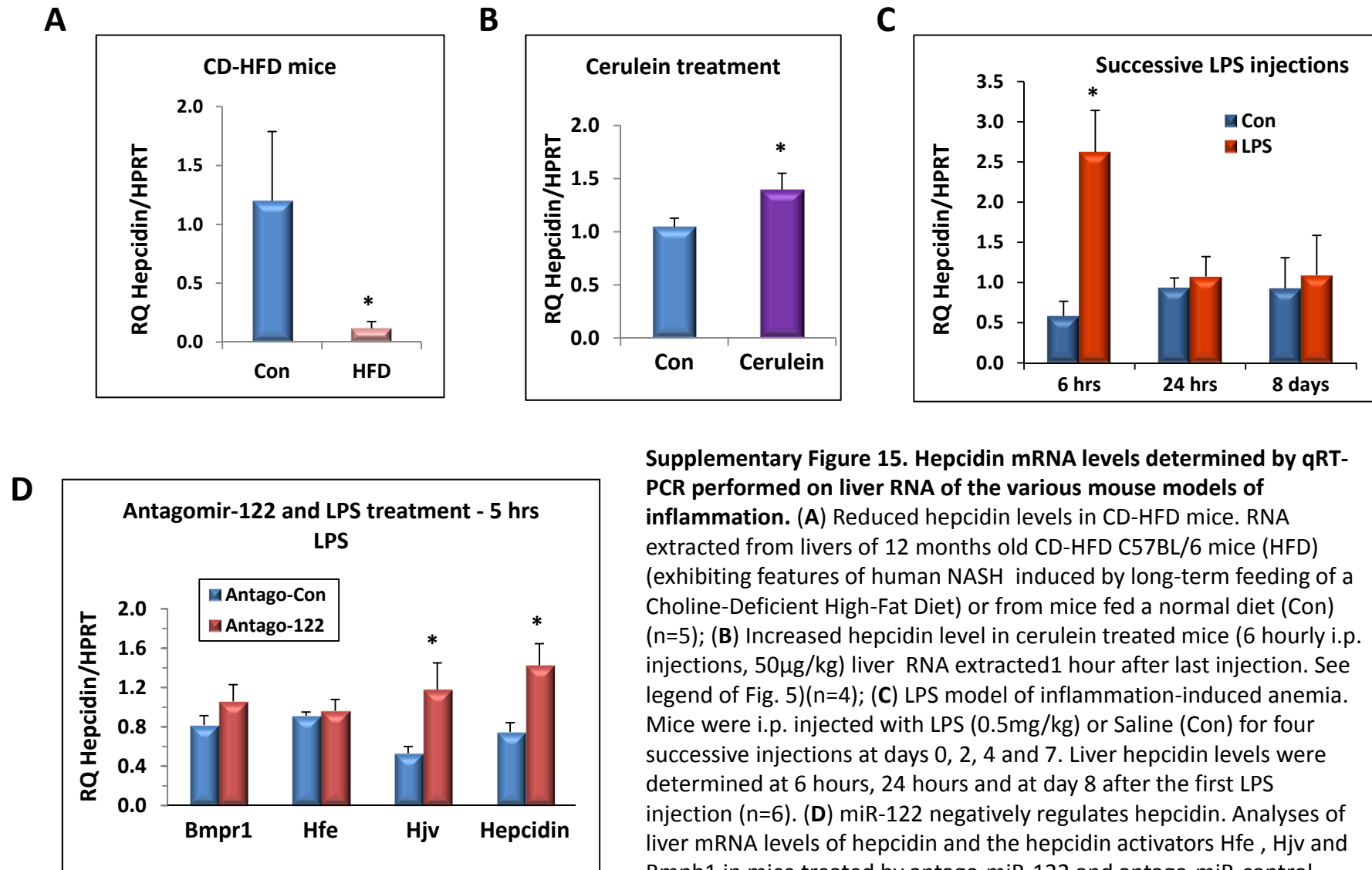
**Supplementary Figure 12. Inhibition of miR-122 does not affect spleen size or weight in antagomiR-122 and LPS-treated mice.** Mice (C57Bl/6) were i.v. hydrodynamically injected with antagomiR-122 or antagomiR-Scr as control (5 $\mu$ g/mouse) 3 days before and one day after the first LPS injection (0.5 ug/gr). Two additional LPS injections were administered at days 2 and 4 (see experimental design in Figure 7C). Mice spleens were measured at day 7 after the first LPS injection for their length (**A**) and their weight (**B**).



**Supplementary Figure 13. GFP Immunofluorescence staining of a paraffin embedded liver tissue.** The miR-122 promoter GFP reporter plasmid (10 ug) was administered into mice by hydrodynamic tail vein injection. One day later, LPS (1 mg/kg) was i.p. injected and the mice were sacrificed 24 hours later. Liver sections were immuno-stained with Anti-GFP antibody. The figure demonstrates that plasmid GFP, driven by the miR-122 promoter, is expressed in hepatocytes and is significantly induced by LPS.



**Supplementary Figure 14. Chromatin immunoprecipitation (ChIP) assay.** Huh7 cells ( $1 \times 10^7$ ) were treated with TNF $\alpha$  (5ng/ml) for 2 or for 16 hrs. Cells were fixed with 1% formaldehyde, lysed and the chromatin was sheared by sonication for 15 minutes. The chromatin was then immunoprecipitated using the anti-p65 antibody (ab7970 abcam). Real-time PCRs were performed to quantify the relative enrichment of immunoprecipitated DNA using primers shown in Supplementary Table 2. The enrichment of each target gene was calculated using the GAPDH as a reference for nonspecific DNA, and taking into account the amount of input. Data are expressed as fold change relative to unstimulated cells.



**Supplementary Figure 15. Hepcidin mRNA levels determined by qRT-PCR performed on liver RNA of the various mouse models of inflammation.** (A) Reduced hepcidin levels in CD-HFD mice. RNA extracted from livers of 12 months old CD-HFD C57BL/6 mice (HFD) (exhibiting features of human NASH induced by long-term feeding of a Choline-Deficient High-Fat Diet) or from mice fed a normal diet (Con) (n=5); (B) Increased hepcidin level in cerulein treated mice (6 hourly i.p. injections, 50 $\mu$ g/kg) liver RNA extracted 1 hour after last injection. See legend of Fig. 5)(n=4); (C) LPS model of inflammation-induced anemia. Mice were i.p. injected with LPS (0.5mg/kg) or Saline (Con) for four successive injections at days 0, 2, 4 and 7. Liver hepcidin levels were determined at 6 hours, 24 hours and at day 8 after the first LPS injection (n=6). (D) miR-122 negatively regulates hepcidin. Analyses of liver mRNA levels of hepcidin and the hepcidin activators Hfe, HJV and Bmp1 in mice treated by antago-miR-122 and antago-miR-control followed by LPS injection. RNA extracted 5 hours after LPS injection (see experimental design in the legend of Fig. 7).

**Supplementary Table 1. Primers used for characterization of pri-miR-122**

Primer number	Sequence (5'→3')	Direction	Purpose	Product length (bp)
P1	GTTATGAGTGCAAAAGAGCCAG	Reverse	Hybridization Probe Intron2 + Exon3	1260
P2	TGCAAGTCCAGCTTGAAGAGGG	Forward		
P3	TTTACCTATAAGGTTGCTCATAGTGCC	Reverse	Hybridization Probe Intron1	466
P4	GATGGGTTCCAACCTTCCC	Forward		
P5	GCTGTCAACGATACGCTACGTAACGGCATGACAGTG(T) <sub>24</sub>	Reverse	cDNA (Invitrogen 3'-RACE)	
P6	AAGGATTGCCTAGCAGTAGC	Reverse	PCR Exon2-3	384
P7	CATGGAGAAGTGGAGGATGC	Forward		
P8	GGAAGAAACAGTGAGAGGTG	Reverse	PCR Exon1-2	210
P9	GCCTTGGACTGAGAGGACCG	Forward		
P10	GCTGTCAACGATACGCTACGTAACG	Reverse	3'-RACE 1st PCR	
P11	CTGGTGTGTTGTGTCTAACTATCAAACGCC	Forward		
P12	CGCTACGTAACGGCATGACAGTG	Reverse	3'-RACE 2nd PCR	180
P13	AATACGTA CTAGGCAATCC	Forward		

**Table S2. Primers for real-time PCR**

Gene	Direction	Sequence (5'→3')
Human HPRT	forward	GGACAGGACTGAACGTCTTGC
	reverse	CAACACTTCGTGGGGTCCTT
Human EPO	forward	GTCCCAGACACCAAAGTTAATTTTC
	reverse	GCCCTGCCAGACTTCTAC
Human pri-miR-122	forward	GCCTTGGACTGAGAGGACCG
	reverse	GGAAGAAACAGTGAGAGGTG
Mouse HPRT	forward	GCGATGATGAACCAGGTTATGA
	reverse	ATCTCGAGCAAGTCTTTTCAGTCCT
Mouse EPO	forward	CTTCACTGCTTCGGGTAAGTGG
	reverse	GTGTACAGCTTCAGTTTCCCC
Mouse pre-miR-122	forward	CCATCAAACGCCATTATCACACTA
	reverse	CACACAATGGAGAACTCTAGCACAA
Mouse TNF $\alpha$	forward	CTGTAGCCCACGTCGTAGCAA
	reverse	CTGGCACCAGTCTAGTTGGTTGTTTC
miR-122	forward	TGGAGTGTGACAATGGTGTGTTG
miR-18a	forward	TAAGGTGCATCTAGTGCAGATAG
miR-16	forward	TAGCAGCACGTAATATTGGCG
RNU-44	forward	CCUGGAUGAUGAUAGCAAUUGCUGACUGAACUGAAG GUCUUAUUUAGCUCUAACUGACU
RNU-6	forward	GUGCUCGCUUCGGCAGCACAUUACUAAAAUUGGAAC GAUACAGAGAAGAUUAGCAUGGCCUUGCGCAAGGAU GACACGCAAAUUCGUGAAGCGUCCAUUUUU
Cel-miR-39-3P	forward	TCACCGGGTGTAAATCAGCTTG
mouse Hfe	forward	CACCGTCTGTGCCATCTTCTT
	reverse	ACATAGCCACCCATGGTTCTT
mouse Hvj	forward	CAGCTCCCCGGTTTCGT
	reverse	TGGTAGACTTTCTGGTCAATGCA
mouse Bmpr1a	forward	CAGTTTTATCTAGCCACATCTCTGA
	reverse	GGGAGGCTTCCTTACAGAACA
Mouse Hepcidin	forward	CTGAGCAGCACCTATCTC
	reverse	TGGCTCTAGGCTATGTTTTGC
<b>Primers for CHIP assay</b>		
human GAPDH	forward	TCTGCTGTAGGCTCATTTCAG
	reverse	TCACCTGATGATCTTGAGGCTG
IL-8	forward	AGAAAACCTTCGTCACTACTCCG
	reverse	AGAGGAAATCCACGATTTGC
IkB $\alpha$	forward	GGAGTTTCTCCGATGAAC
	reverse	TCAGGCTCGGGGAATTTCC
human miR-122 promoter	forward	TGCCTGCTGGCCGCACACCC
	reverse	CAAAACACTCAGCAAGATTGG

Supplementary Table 3. Primer for plasmids constructs

Primer number	Direction	Sequence (5'→3') <sup>ab</sup>	Restriction Sites at 5'-end	Cloning
P20	forward	<i>GACACGCGTAGTCAACATGGTGAAACCC</i>	MluI	miR-122 promoter (-900)
P21	reverse	<b>GACCTGGACAGAGGCATGCCAAAGG</b>		
P22	forward	<i>CTCTTACGCGTGACCTGTCTTCTCTGCCTCGG</i>	MluI	miR-122 promoter (-250)
P23	forward	<b>AATGGACTCTCGAGTCTTGCTGAGTGTG</b>		mutate NF-kB site in mir-122 promoter
P24	reverse	<b>CAAGACTCGAGAGTCCATTCTCTGCTGAG</b>		
P25	forward	<i>ATATTTGGTACCCTGCCACTCTAGTAC</i>	KpnI	human IL-8 promoter
P26	reverse	<i>ATATTTAAGCTTGTGTGCTCTGCTGTCTC</i>	HindIII	
P27	forward	<i>GCTAGCCTCGAGTGACCAGGTGTGTCCACC</i>	NheI XhoI	human EPO 3'-UTR
P28-2	reverse (2 miR-122 sites)	<i>AACCTGCAGGTCGACCCTGAGATGTCATTGCTG</i>	PstI Sall	
P28-3	reverse (3 miR-122 sites)	<i>AACCTGCAGGTCGACCCTGTCTTCATGGTCCCAC</i>	PstI Sall	
P29	forward	<i>GCTAGCCTCGAGGTGACATGCTGCTGCCACC</i>	NheI XhoI	mouse EPO 3'-UTR
P30	reverse	<i>AACCTGCAGGTCGACAGCTCTGGGAAGTTCTTCTG</i>	PstI Sall	
P31	forward	<i>TAACCAGAGCTCCTCTTCGTCTTAACCACG</i>	SacI	human ALDOA1 3'-UTR
P32	reverse	<i>ACCAATCTAGAGCTGTTTATTTGGCAG</i>	XbaI	
P33	forward	<i>CCTCTGAGCTCCAAAGCCCGAGAGAGTG</i>	SacI	human DNMT1 3'-UTR
P34	reverse	<i>ATGACTCTAGAAGAATGCACAAAGTACTGC</i>	XbaI	
P35	forward	<i>TTAACCGGTACCTCAGCAGAGGAATGGAC</i>	KpnI	miR-122 promoter (-190)
P36	forward	<i>TTAACCGGTACCGTGTGTTGACCAAAGGTGG</i>	KpnI	miR-122 promoter (-150)
P37	forward	<i>TTA CCGGTACCCCTAAGGTCGTGCCCTCC</i>	KpnI	miR-122 promoter (-120)

<sup>a</sup> Bases written in italic were added to the primer 5'-end to add a restriction site.

<sup>b</sup> Bases shown in red were substituted in order to mutate the NF-kB site in the miR-122 promoter

**Supplementary Table 4. Changes in EPO and miR-122 levels in human patients during acute inflammation conditions**

Disease	Number of patients	Age	miR-122 ↑ EPO ↓	miR-122 ↓ EPO ↑	No change miR-122/EPO	miR-122 ↓ EPO ↓
Acute Cholecystitis	10	18-71	7	2	1	
Pancreatitis	1	71	1			
Periappendicular abscess	1	26	1			
Pneumonia	2	52, 82	2			
Urinary tract infection	1	91	1			
Cholangitis	1	53		1		
Diverticulitis	1	68				1

↑ Upregulated

↓ Down regulated

Supplementary Table 3. Primer for plasmids constructs

Primer number	Direction	Sequence (5'→3') <sup>ab</sup>	Restriction Sites at 5'-end	Cloning
P20	forward	<i>GACACGCGTAGTCAACATGGT</i> GAAACCC	MluI	miR-122 promoter (-900)
P21	reverse	<b>GACCTGGACAGAGGCATGCCAAAGG</b>		
P22	forward	<i>CTCTTACGCGTGACCTGTCTTCTCTGCCTCGG</i>	MluI	miR-122 promoter (-250)
P23	forward	<b>AATGGACTCTCGAGTCTTGCTGAGTGTG</b>		mutate NF-kB site in mir-122 promoter
P24	reverse	<b>CAAGACTCGAGAGTCCATTCTCTGCTGAG</b>		
P25	forward	<i>ATATTTGGTACCCTGCCACTCTAGTAC</i>	KpnI	human IL-8 promoter
P26	reverse	<i>ATATTTAAGCTTGTGTGCTCTGCTGTCTC</i>	HindIII	
P27	forward	<i>GCTAGCCTCGAGTGACCAGGTGTGTCCACC</i>	NheI XhoI	human EPO 3'-UTR
P28-2	reverse (2 miR-122 sites)	<i>AACCTGCAGGTCGACCCTGAGATGTCATTGCTG</i>	PstI Sall	
P28-3	reverse (3 miR-122 sites)	<i>AACCTGCAGGTCGACCCTGTCTTCATGGTCCAC</i>	PstI Sall	
P29	forward	<i>GCTAGCCTCGAGGTGACATGCTGCTGCCACC</i>	NheI XhoI	mouse EPO 3'-UTR
P30	reverse	<i>AACCTGCAGGTCGACAGCTCTGGGAAGTTCTTCTG</i>	PstI Sall	
P31	forward	<i>TAACCAGAGCTCCTCTTCGTCTCTAACCACG</i>	SacI	human ALDOA1 3'-UTR
P32	reverse	<i>ACCAATCTAGAGCTGTTTATTTGGCAG</i>	XbaI	
P33	forward	<i>CCTCTGAGCTCCAAAGCCCGAGAGAGTG</i>	SacI	human DNMT1 3'-UTR
P34	reverse	<i>ATGACTCTAGAAGAATGCACAAAGTACTGC</i>	XbaI	
P35	forward	<i>TTAACCAGGTACCTCAGCAGAGGAATGGAC</i>	KpnI	miR-122 promoter (-190)
P36	forward	<i>TTAACCAGGTACCGTGTGTTGACCAAAGGTGG</i>	KpnI	miR-122 promoter (-150)
P37	forward	<i>TTA CCGGTACCCCTAAGGTCGTGCCCTCC</i>	KpnI	miR-122 promoter (-120)

<sup>a</sup> Bases written in italic were added to the primer 5'-end to add a restriction site.

<sup>b</sup> Bases shown in red were substituted in order to mutate the NF-kB site in the miR-122 promoter